Heat Flux, Erosion Rate, Implantation, and Damage Rate to the Walls of the EG&G Fusion Blanket Test Module

A.M. Hassanein, G.L. Kulcinski, and G.R. Longhurst

October 1980

UWFDM-389

Nuclear Technology/Fusion 2, 120 (Jan. 1982).

FUSION TECHNOLOGY INSTITUTE

UNIVERSITY OF WISCONSIN

MADISON WISCONSIN

Heat Flux, Erosion Rate, Implantation, and Damage Rate to the Walls of the EG&G Fusion Blanket Test Module

A.M. Hassanein, G.L. Kulcinski, and G.R. Longhurst

Fusion Technology Institute
University of Wisconsin
1500 Engineering Drive
Madison, WI 53706

http://fti.neep.wisc.edu

October 1980

UWFDM-389

Nuclear Technology/Fusion 2, 120 (Jan. 1982).

Heat Flux, Erosion Rate, Implantation, and Damage Rate to the Walls of the EG&G Fusion Blanket Test Module

A. M. Hassanein

G. L. Kulcinski

G. R. Longhurst*

Fusion Engineering Program
Nuclear Engineering Department
University of Wisconsin
Madison, WI 53706

October 1980

UWFDM-389

*EG & G Idaho, Idaho Falls.

Heat Flux, Erosion Rate, Implantation, and Damage Rate to the Walls of the EG&G Fusion Blanket Test Module

A. M. Hassanein

G. L. Kulcinski

G. R. Longhurst*

Fusion Engineering Program
Nuclear Engineering Department
University of Wisconsin
Madison, WI 53706

October 1980

Number of Pages: 36
Number of Tables: 0
Number of Figures: 23

---

*EG & G Idaho, Idaho Falls.

I. Introduction

It has recently been proposed by Hsu and Miller[1] that one can use a thermal fission reactor to produce bulk neutron and surface effects which are similar to those experienced by the first walls in a DT fusion reactor. The main idea is to use the (n,α) reaction in Ni-59 to produce high internal helium contents in the metal while using the $He^3(n,P)T$ reaction in the gas surrounding the specimen to produce an external heat and particle flux. The helium-3 gas would be contained in an annulus around the material to be tested as depicted in Fig. 1. The pressure of the gas could be varied to change the particle flux and energy which, in turn, would change the heat flux, the erosion rate, and the displacement rate in the test material.

The basic problem is to calculate the partitioning of the reaction energy; i.e., how much of the recoil energy is deposited on the wall? It is also of interest to know the energy spectrum of the protons and tritium ions as a result of the reaction:

$$n + He^3 \rightarrow p(E_o = 0.57 \text{ MeV}) + T(E_o = 0.19 \text{ MeV}) \qquad (1)$$

as they hit the wall.

The object of this study is:

(1) To calculate the energy spectrum of the charged particles at the inner first wall of a 1 cm thick gap filled with various pressures of He^3 gas;

(2) To calculate the total heat flux at the same inner wall for typical ETR operating conditions;

(3) To calculate the total erosion rate at this inner wall;

(4) To calculate the damage rate (dpa/sec) in the stainless steel inner wall;

Figure 1

Simplified Schematic of Fusion Blanket Test Module Proposed by EG&G To Be Placed in Thermal Fission Test Reactor

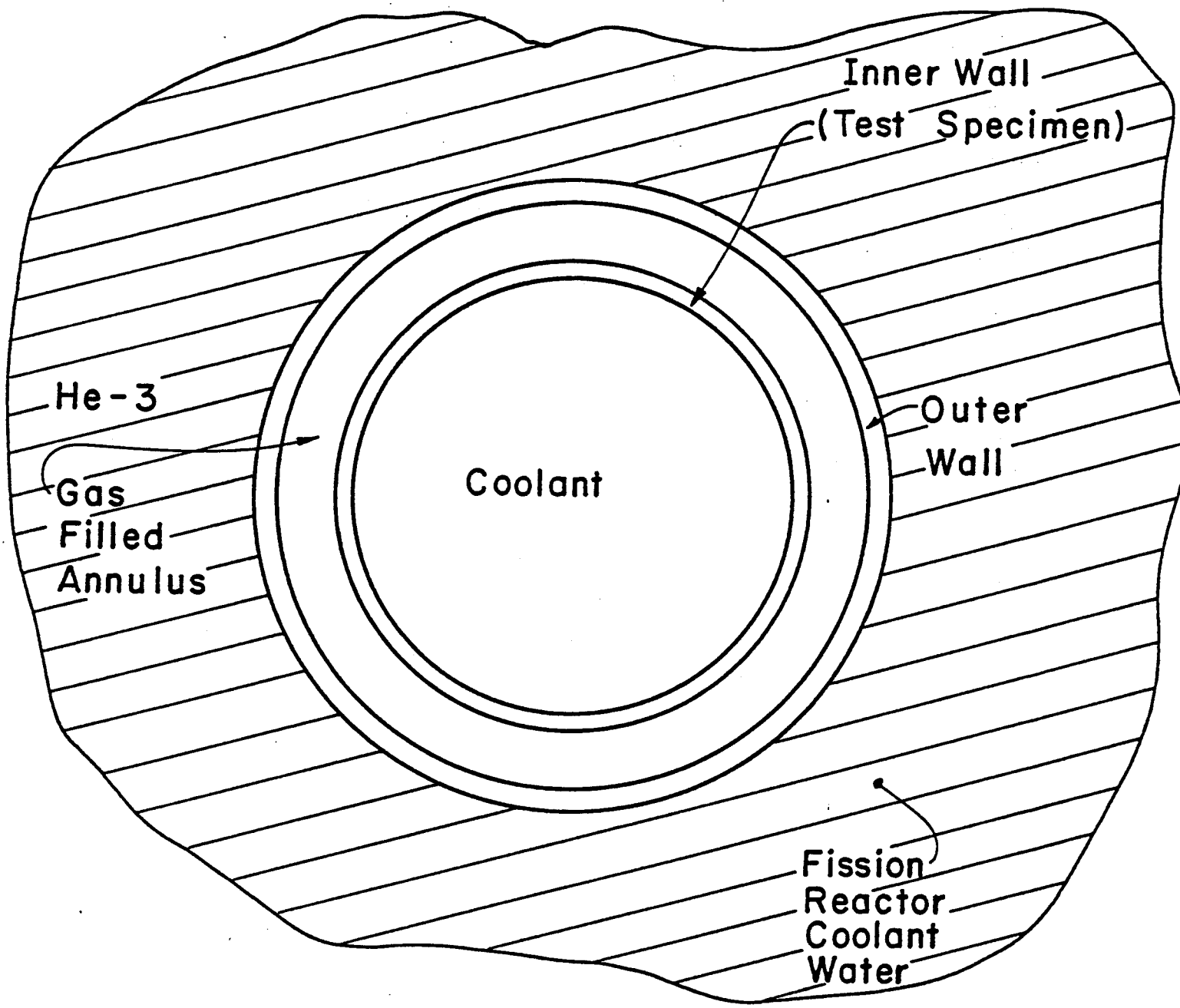

(5) To calculate the implantation of protons and tritium in the stainless steel inner wall;

and

(6) To repeat the above calculations on the outer wall as well as on the inner one.

II. Calculational Model

A. General Features

In this study, the problem will be modeled as an infinite slab with 1 cm thick gas gap although other thicknesses could be used. An exponential law for the $He^3(n,p)T$ reaction rate distribution will be assumed.

Consider a layer of thickness dx where protons and tritium are produced at rate given by:

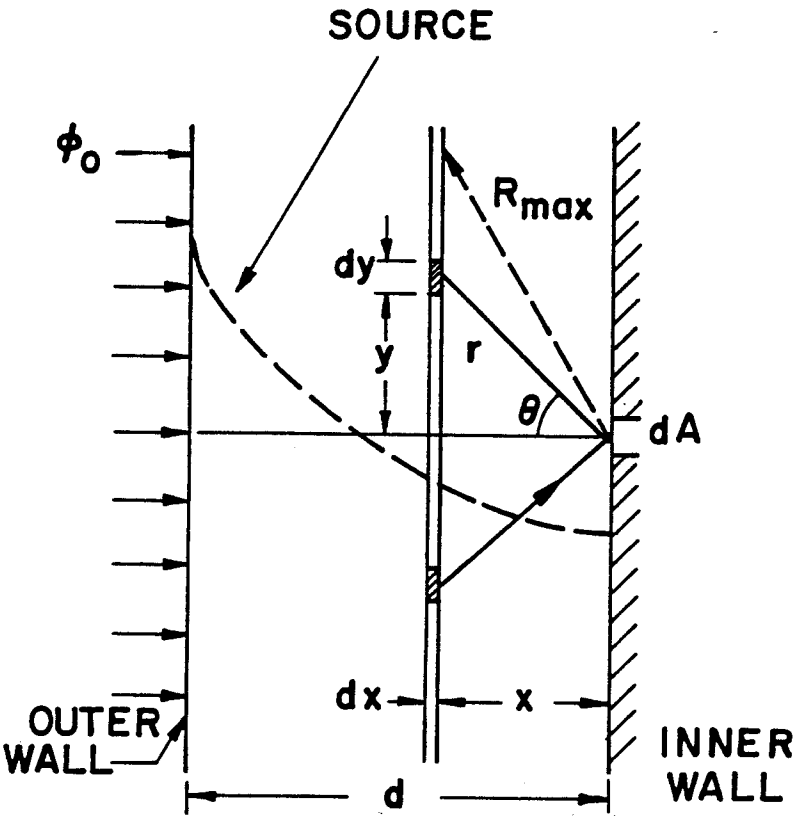

FIGURE (2)

$$R = \Sigma \phi_o e^{-\Sigma(d-x)} \text{ cm}^{-3} \text{ sec}^{-1} \qquad (2)$$

where Σ is the total absorption cross section (cm^{-1}),

ϕ_o is the neutron flux incident on the outer wall (# cm^{-2} sec^{-1}),

d is the thickness of the gas gap.

These are assumed produced isotropically at every location y (as shown in Fig. 2).

The fraction of the particles produced in the annular ring (defined by x, y, dx, dy) which start toward dA is:

$$f = \frac{dA \cos\theta}{4\pi r^2} \quad . \tag{3}$$

Then the particle flux from this ring going towards dA is given by:

$$dF_p = \Sigma \phi_o e^{-\Sigma(d-x)} \cdot 2\pi y \, dy \frac{dA}{4\pi r^2} \frac{x}{\sqrt{x^2 + y^2}} dx \quad . \tag{4}$$

To get the total number of particles produced at x from the volume element between x and x + dx, we integrate over the annular ring:

$$F_p/dA = \frac{1}{2} \Sigma \phi_o e^{-\Sigma(d-x)} x \, dx \int_o^{\sqrt{R_{max}^2 - x^2}} \frac{y}{(x^2 + y^2)^{3/2}} dy \quad . \tag{5}$$

R_{max} is the range of the particles at the corresponding He^3 gas pressure

$x^2 + y^2 = r^2$

and $y \, dy = r \, dr$ (at constant x) .

The flux of particles per unit area is then:

$$\begin{aligned} F_p/dA &= \frac{1}{2} \Sigma \phi_o e^{-\Sigma(d-x)} x \, dx \int_{r=x}^{r=R_{max}} \frac{dr}{r^2} \\ &= \frac{1}{2} \Sigma \phi_o e^{-\Sigma(d-x)} \left(1 - \frac{x}{R_{max}}\right) dx \quad . \end{aligned} \tag{6}$$

For the rest of this paper, the particle and heat fluxes will be normalized to the units of $\Sigma\ \phi_o$ (where ϕ_o is the flux of incident neutrons at the outside wall, assuming no shielding from this wall), i.e.

$$F_{p_a} = \frac{1}{2} e^{-\Sigma(d-x)} \left(1 - \frac{x}{R_{max}}\right) dx \tag{7}$$

and the units are $\left(\frac{\text{particles}}{\text{cm}^2 \cdot \text{sec}}\right) / \left(\frac{\text{Reaction}}{\text{cm}^3 \cdot \text{sec}}\right)$.

To obtain the total number of particles that reach the area element dA from all gas regions, we integrate over all the volume,

$$F_{tot} = \int_o^L F_{p_a}\, dx \qquad (F_{p_a} \text{ flux from region between } x,\ x + dx) \tag{8}$$

where L is the lesser between R_{max} and d, i.e.,

$$F_{tot} = \int_o^L \frac{1}{2} e^{-\Sigma(d-x)} \left(1 - \frac{x}{R_{max}}\right) dx \quad . \tag{9}$$

In fact, this last integral can be solved analytically, and the result is given by:

$$F_{tot} = \frac{1}{2\Sigma} \left[e^{\Sigma(L-d)} \left(1 + \frac{1}{\Sigma\ R_{max}} - \frac{L}{R_{max}}\right) - e^{-\Sigma d} \left(1 + \frac{1}{\Sigma\ R_{max}}\right)\right] \tag{10}$$

where again L is the lesser between d and R_{max}. Again, it should be noticed that F_{tot} is normalized to the units of $\Sigma\ \phi_o$.

The total flux given by the last integral is strongly dependent on the He^3 gas pressure in the gap. This pressure dependence enters through the

absorption cross section, Σ, and the range of the particles in the gas, i.e. R_{max}.

B. Heat Flux

The heat flux to the inner wall from the volume element between x and x + dx is given by:

$$\text{Heat flux} = \frac{1}{2} e^{-\Sigma(d-x)} \; x \; dx \int_{r=x}^{R_{max}} E(r) \cdot \frac{dr}{r^2} \quad \left[\frac{\text{watt}}{\text{cm}^2} / (\text{reaction/cm}^3 \cdot \text{sec})\right] \tag{11}$$

and the total heat flux is given by:

$$= \frac{1}{2} \int_{x=0}^{L} x \; e^{-\Sigma(d-x)} \int_{r=x}^{R_{max}} E(r) \frac{dr}{r^2} \, dx \tag{12}$$

where E(r) is the energy that reaches the wall from particles born with energy E_0 at the volume element dx and at a distance r from the first wall.

To simplify the last integral, we can calculate an average distance $\bar{r}$ (defined as the average distance travelled by those particles born within the slab volume element x and x + dx). Then we calculate the energy of the particles that traverse this distance, i.e. $E(\bar{r})$. Then, the total heat flux will be given by

$$\begin{aligned} &= \frac{1}{2} \int_{0}^{L} e^{-\Sigma(d-x)} \; x \; E(\bar{r}) \int_{r=x}^{R_{max}} \frac{dr}{r^2} \, dx \\ &= \frac{1}{2} \int_{0}^{L} e^{-\Sigma(d-x)} \left(1 - \frac{x}{R_{max}}\right) E(\bar{r} = f(x)) \, dx \; . \end{aligned} \tag{13}$$

To get $\bar{r}$, we have to calculate the average distance travelled over the solid angle $d\Omega$, i.e.,

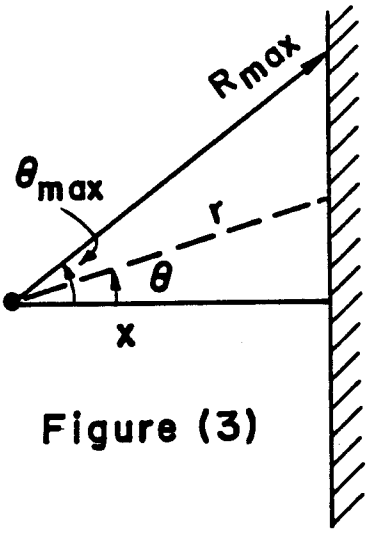

Figure (3)

$$\bar{r} = \frac{\int_0^{\theta_{max}} r \, d\Omega}{\int_0^{\theta_{max}} d\Omega} \tag{14}$$

where $d\Omega = 2\pi \sin\theta \, d\theta$. Substituting for $r = \frac{x}{\cos\theta}$ (as shown in Fig. 3) we find,

$$\bar{r} = \frac{\int_0^{\theta_{max}} \frac{x}{\cos\theta} 2\pi \sin\theta \, d\theta}{\int_0^{\theta_{max}} 2\pi \sin\theta \, d\theta}$$

$$= \frac{x \int_0^{\theta_{max}} \tan\theta \, d\theta}{\int_0^{\theta_{max}} \sin\theta \, d\theta}$$

$$= x \frac{\ln \sec\theta_{max}}{1 - \cos\theta_{max}} \, . \tag{15}$$

The following substitution $\cos \theta_{max} = \frac{x}{R_{max}}$ yields,

$$\bar{r} = x \frac{\ln (R_{max}/x)}{(1 - \frac{x}{R_{max}})} \quad . \tag{16}$$

This value of $\bar{r}$ can then be substituted into Eq. 13. If the energy $E(\bar{r})$ can be represented by a suitable polynomial or any other function, the entire problem can be done analytically, even without the approximation of $\bar{r}$.

In this study we solved the last integral numerically. The gas zone is broken up into 100 regions (i.e., each with 0.01 cm thickness). The energy of the ions reaching the inner surface was calculated in the following manner. First, the Brice[2] formulation was used to calculate the electronic energy loss rate of the proton and tritium ions in the He^3 gas. Second the formalism of Hunter[3] was used to calculate the energy at any given distance from the point of birth. This method is valid for low atomic weight particles because the electronic loss mechanism is far greater than the nuclear energy loss mechanism down to a few keV.

C. Sputtering Rate

The sputtering rate is the flux of particles at energy $\bar{E}$ times the appropriate sputtering coefficient, S(E). The sputtering coefficients are calculated from the analytical expression given by Smith[4]:

$$S(E) = (20/U_o)\, Z_1^2\, Z_2^2\, \frac{M_1}{M_2}\, \frac{E}{(E + 50\, Z_1 Z_2)^2} \tag{17}$$

where: U_o = surface binding energy,

Z_1, M_1 = charge and mass of incident ion,

Z_2, M_2 = charge and mass of struck ion,

E = energy in eV.

Fitting the above form of the equation to the experimental data of Sigmund[5] gives

$$S(E) = 19.4\, Z_1^2\, Z_2^2\, \frac{M_1}{M_2}\, \frac{E}{(E + 166.8\, Z_1 Z_2)^2} \quad . \tag{18}$$

For protons and tritium ions on Cu the above equation transforms to:

$$S(E) = 0.257\, \frac{E(keV)}{(E + 4.837)^2} \qquad \text{protons} \tag{19}$$

$$S(E) = 0.711\, \frac{E(keV)}{(E + 4.837)^2} \qquad \text{tritium} \quad . \tag{20}$$

Then the total sputtering rate can be given by:

$$= \frac{1}{2} \int_0^L x e^{-\Sigma(d-x)} \int_{r=x}^{R_{max}} S(E(r)) \cdot \frac{dr}{r^2}\, dx \tag{21}$$

and again if we use $E(\bar{r})$, and take it out of the second integral, the total erosion rate in units of [(cm/sec)/(Reaction/cm^3/sec)] will be given by,

$$S_T = \frac{1}{2}\, S_1 \int_0^L e^{-\Sigma(d-x)} \left(1 - \frac{x}{R_{max}}\right) \frac{E(\bar{r})}{(E(\bar{r}) + 4.837)^2}\, dx \tag{22}$$

where: $S_1 = 0.257$ for protons

$S_1 = 0.711$ for tritium.

It should also be noticed that the total erosion rates are normalized to units of $\Sigma\, \phi_o$.

D. Displacement Response

The radiation damage in the first wall of the fusion blanket test module will be due to both neutrons and ion bombardment. The damage production by the ions will be limited to the first few microns near the exposed surface and the spatial extent of the damage will be determined by the amount of energy lost in nuclear collisions at any location.

The amount of displacement damage by ions can be determined at any location in the material at which the energy of the ion is known by[6]

$$\dot{D}(x) = F_p(x) \int_{E_d}^{\Lambda E_i} \sigma(E_i, E)\, \nu(E)\, dE \qquad (23)$$

where: F_p = local ion flux at position x,

E_d = effective displacement energy,

ΛE_i = maximum PKA energy = $\dfrac{4m_1 m_2 E}{(m_1 + m_2)^2}$,

σ = cross section for transfer of energy E to PKA from ion of any E_i,

$\nu(E)$ = number of displaced atoms from PKA of energy E.

The local displacement rate can be estimated by assuming suitable cross sections in the last equation and integrating. The spatial distribution of the damage requires knowledge of the energy at a given location. Again in this section we used the same methods as those used in calculating the energy spectrum on the inner surface of stainless steel through the gas. The cross section used for this study was the same as the one used by Hunter[3].

III. Calculational Procedure

A computer code, A*IDAHO,[7] has been developed to calculate the steady-state values of particle and heat flux to the wall. Erosion rate, implantation of particles, and damage rate of the wall can also be calculated from this code. All these calculations can be done for any value of He^3 gas pressure. Also, the code is capable of doing all the above calculations on the outer wall as well as on the inner one.

Output from this code can be obtained in either tabulated form or in a graphical form. In this paper we will represent graphical results of the above calculations.

IV. Results and Observations

Results of four different pressures, 1, 3, 5, 32.7 atmospheres of He^3 gas in the annulus between the specimen and the outside of the module, will be shown. (The latter number corresponds to 480 psi originally proposed for the experiment.) The variation in the particle flux, heat flux and erosion rate with pressure will be shown both for the inner and outer wall. The results are given in different ways:

A) The differential particle flux as a function of energy to the first inner wall per unit of $\Sigma \phi_0$ for both protons and tritium ions.

B) The differential heat flux to the first inner wall per unit of $\Sigma \phi_0$ as a function of energy for both protons and tritium ions.

C) The concentrations per unit of $\Sigma \phi_0$ of both protons and tritium particles implanted into the stainless steel wall as a function of distance into the inner wall.

D) The damage rate (dpa/sec) per unit of $\Sigma \phi_0$ from both protons and tritium ions as a function of distance into the stainless steel inner wall.

E) The same calculations above but for the outer wall of the blanket test module.

The graphical representation of the results (Figs. 4 through 19) begins by showing the particle and heat flux for both protons and tritium. This is followed by the concentrations of the particles and the displacement rate in the stainless steel wall for both protons and tritium. Then the calculations are repeated for the outer wall of the blanket test module at the same He^3 gas pressure in the annulus. Finally the pressure of the He^3 gas is changed and the above calculations are repeated. Four different pressure cases are presented here, i.e. 1, 3, 5, 32.7 atm of the He^3 gas.

The variations of the total particle flux, total heat flux and the erosion rate with He^3 gas pressure are shown in Figs. 20 through 23 for both protons and tritium. In these calculations we have used $\phi_o = 2.5 \times 10^{14}$ neutrons/cm^2·sec, a typical value for ETR. The results could be easily adjusted to other values characteristic of different reactor environments.

V. Observations

A. Particle and Heat Flux

1. Because of the higher energy of the protons (i.e., longer range) the flux of the protons will be greater than for the tritium ions.
2. The flux of the high energy protons (e.g. 500 keV) is roughly twice those of lower energy (~ 100 keV).
3. The total particle flux on the inside wall is maximum at ~ 4 atm of He^3 gas and it is significantly reduced at 32.7 atm.
4. The heat flux of the protons is much higher than that for tritium since the average energy and particle flux is higher for protons.

Figure 4.

INNER WALL (1.0 ATM)

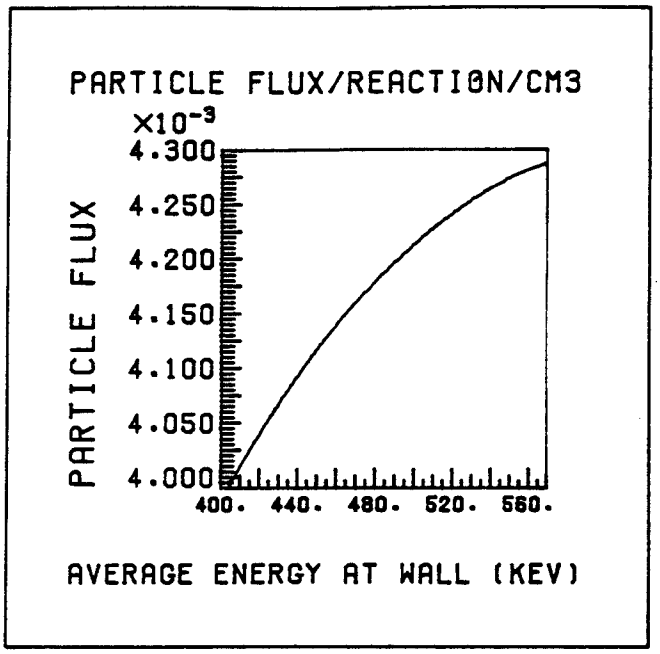

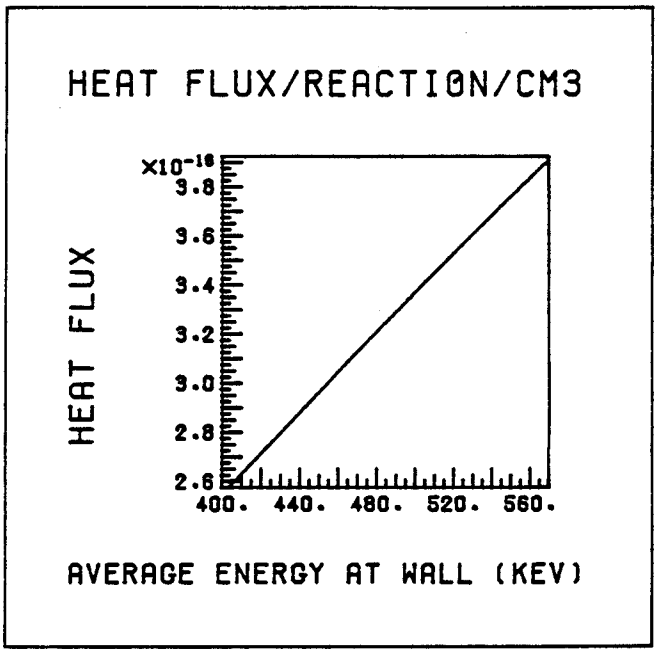

PROTONS

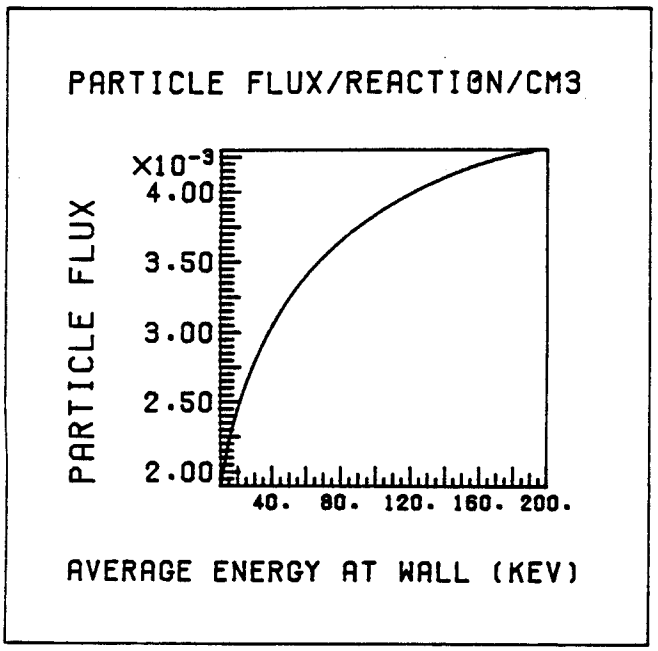

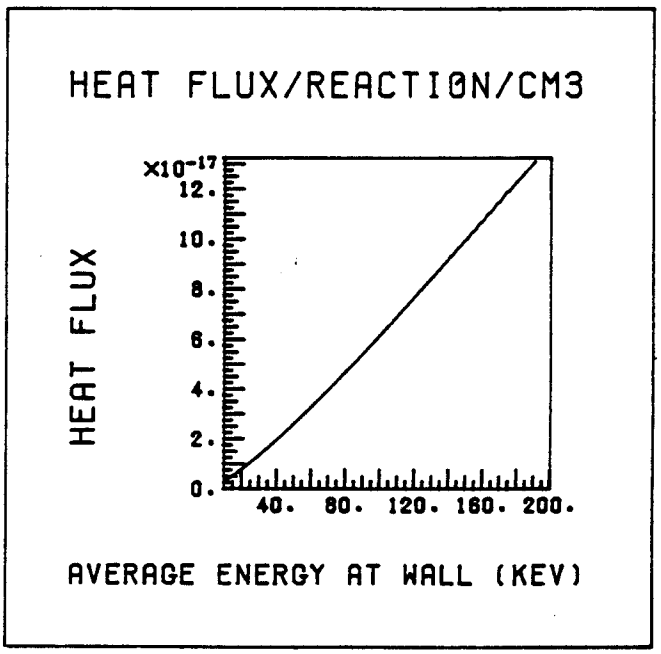

TRITIUM

Figure 5.

INNER WALL (1.0 ATM)

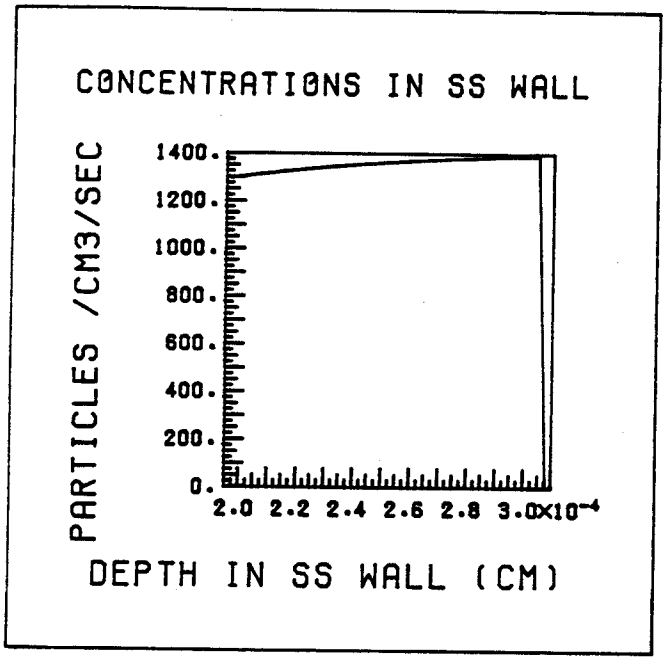

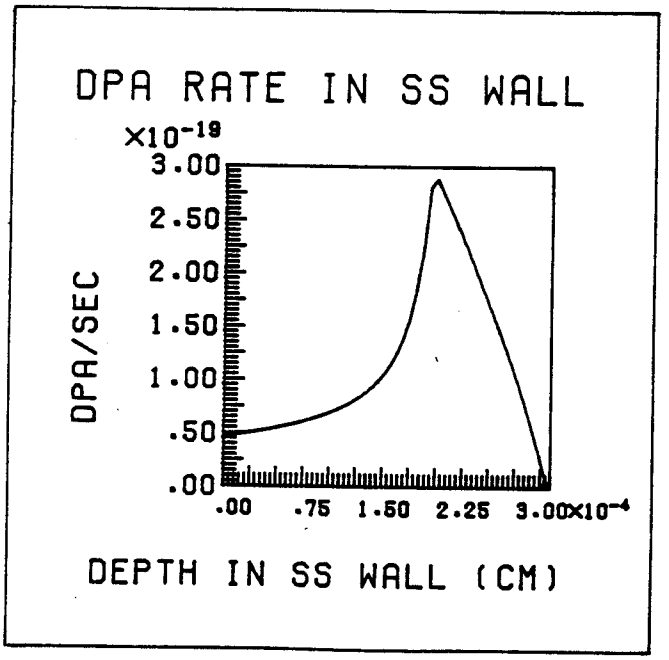

PROTONS

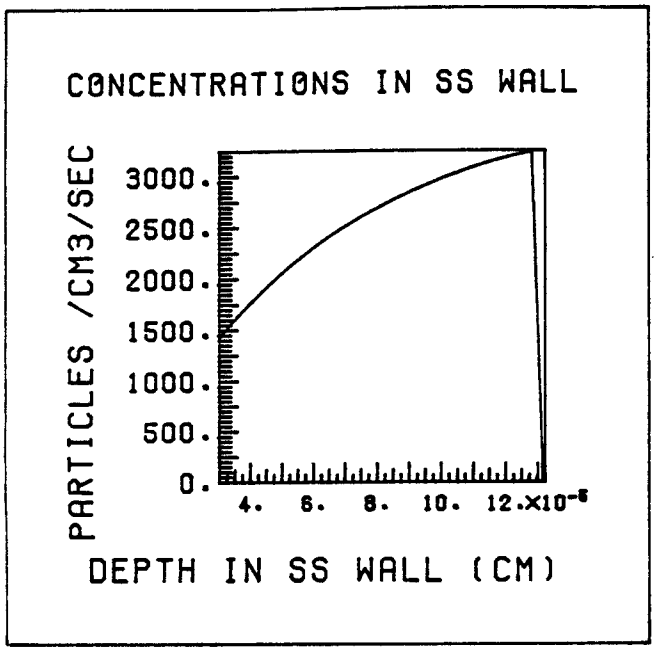

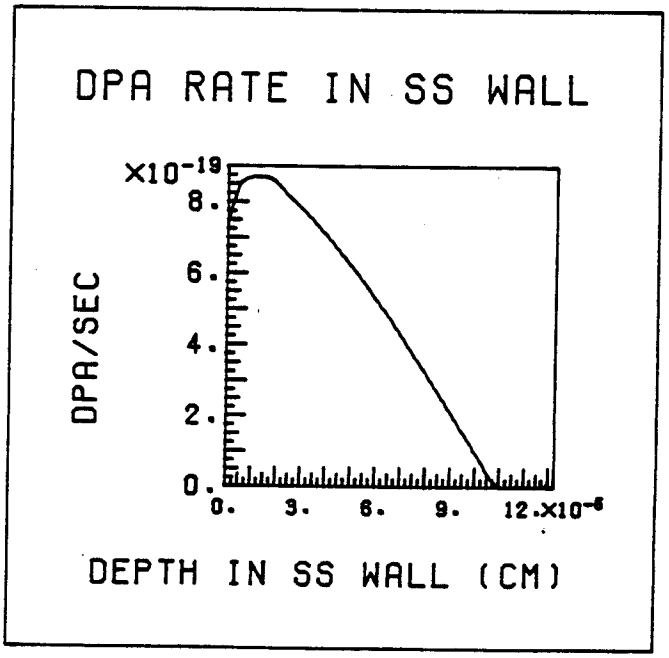

TRITIUM

Figure 6.

OUTER WALL (1.0 ATM)

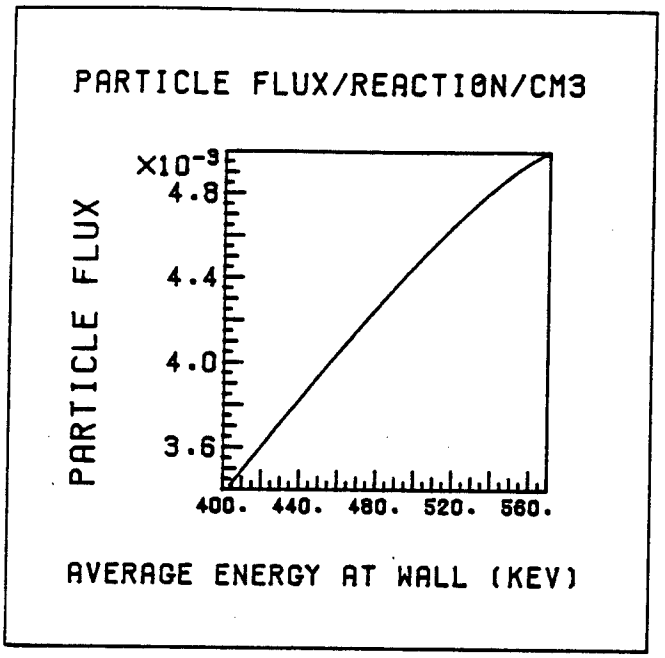

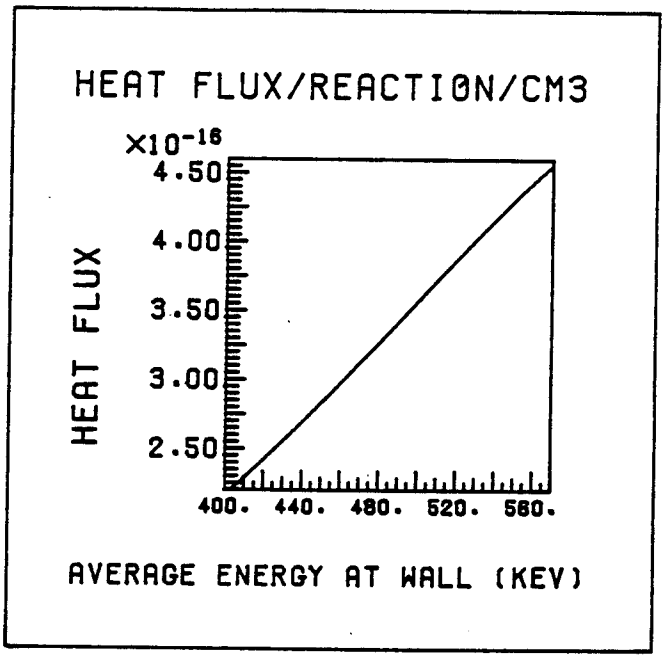

PROTONS

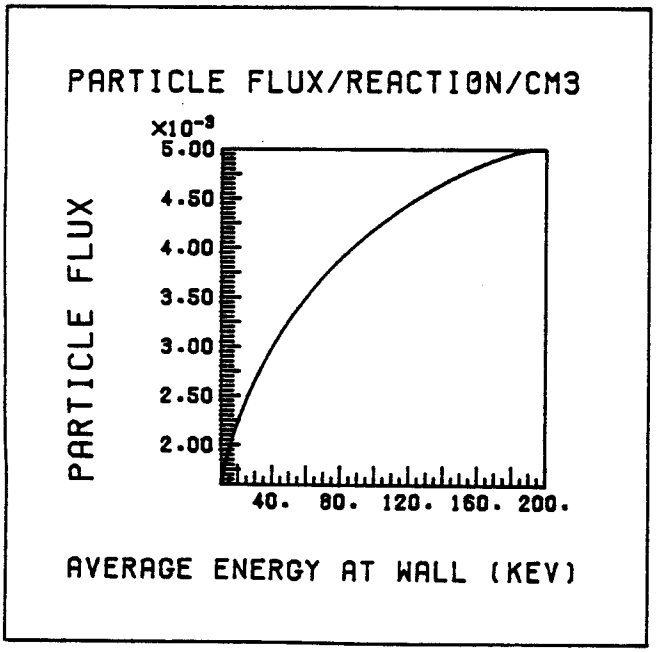

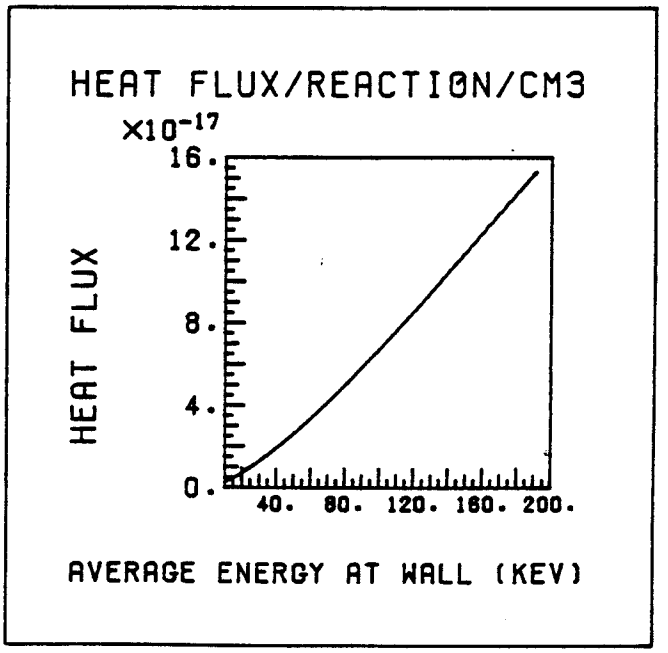

TRITIUM

Figure 7.

OUTER WALL (1.0 ATM)

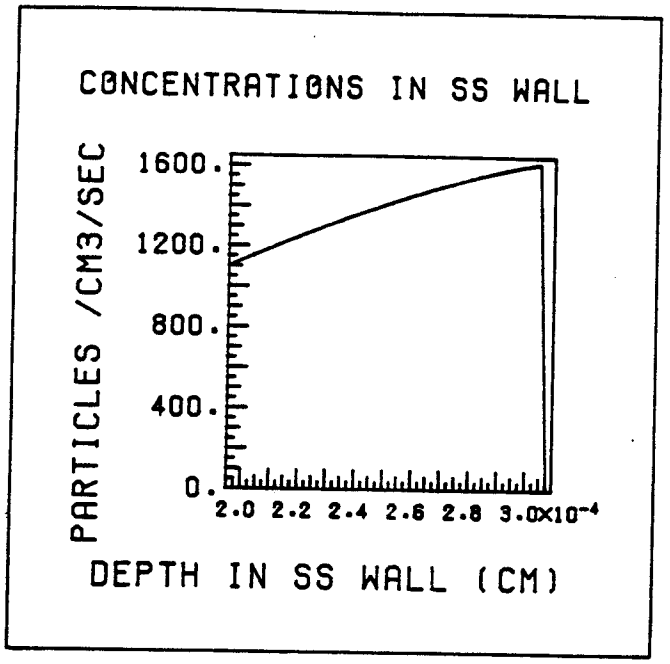

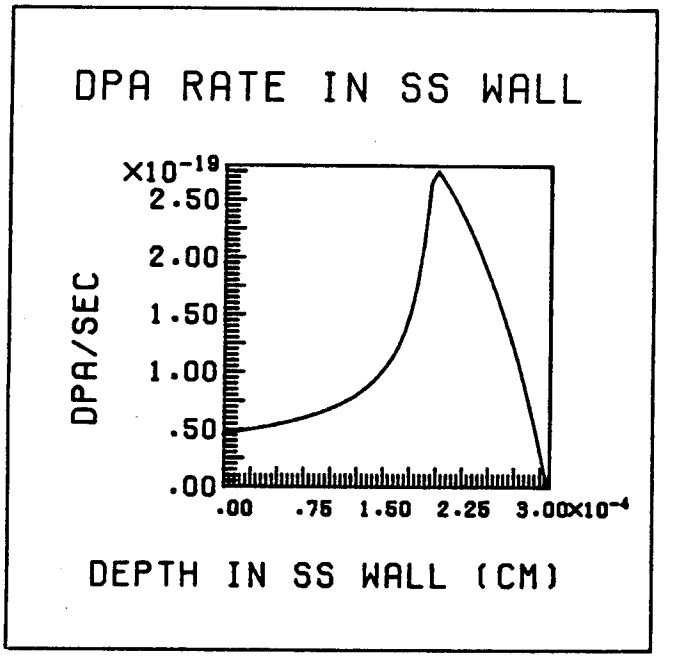

PROTONS

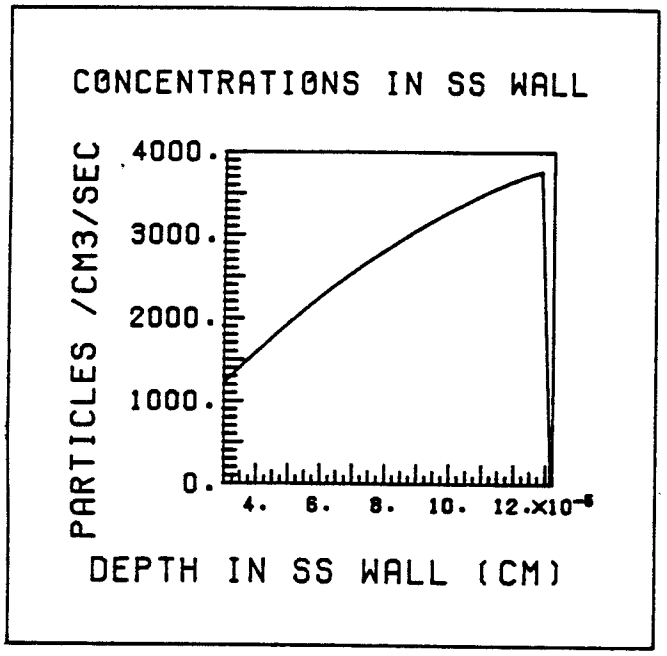

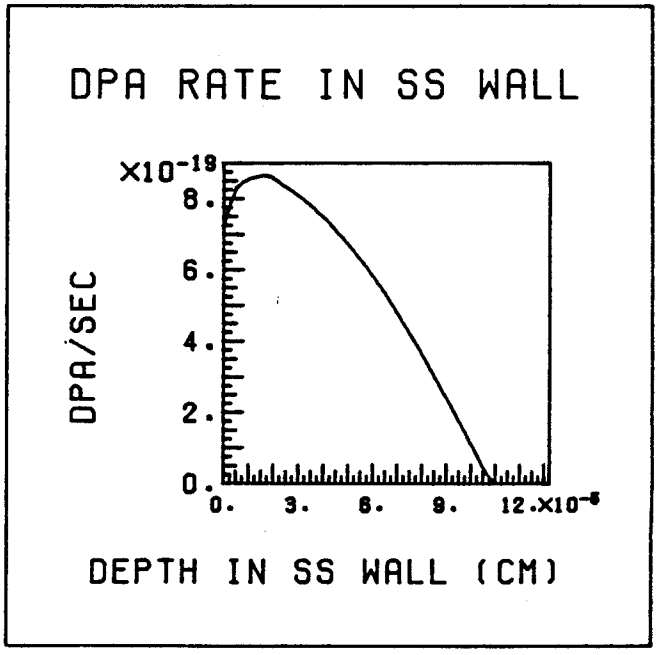

TRITIUM

Figure 8.

INNER WALL (3.0 ATM)

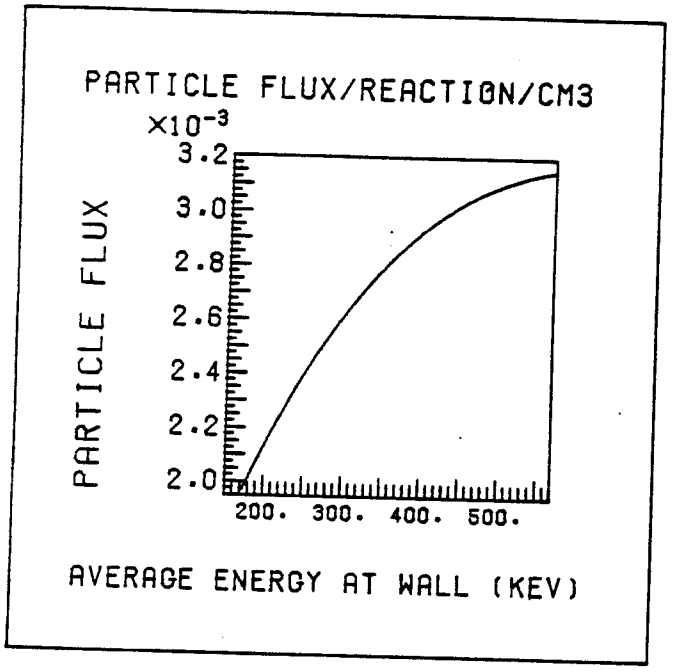

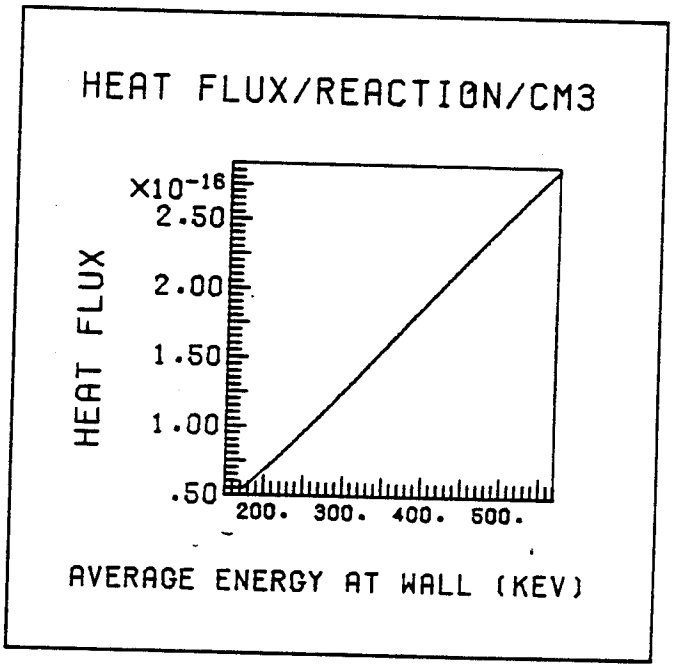

PROTONS

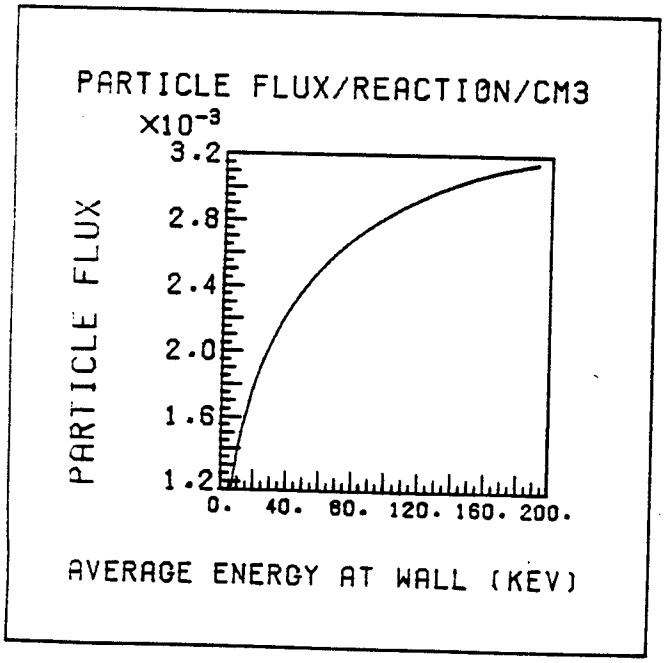

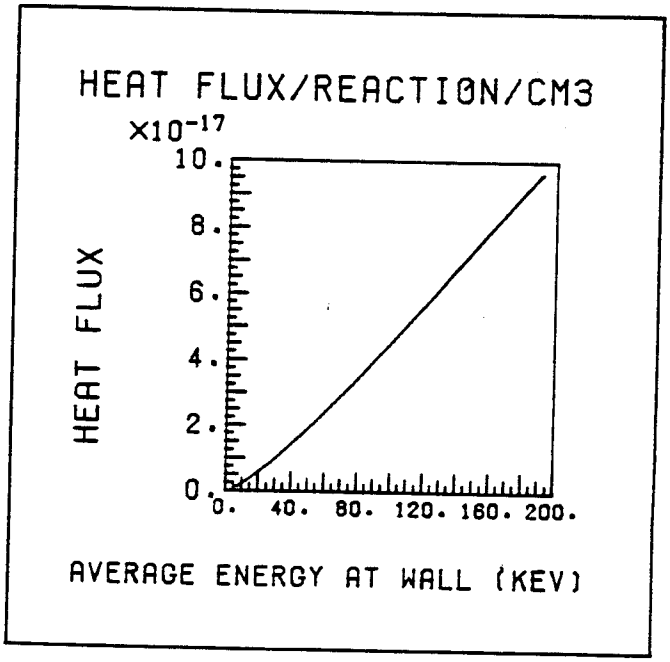

TRITIUM

Figure 9.

INNER WALL (3.0 ATM)

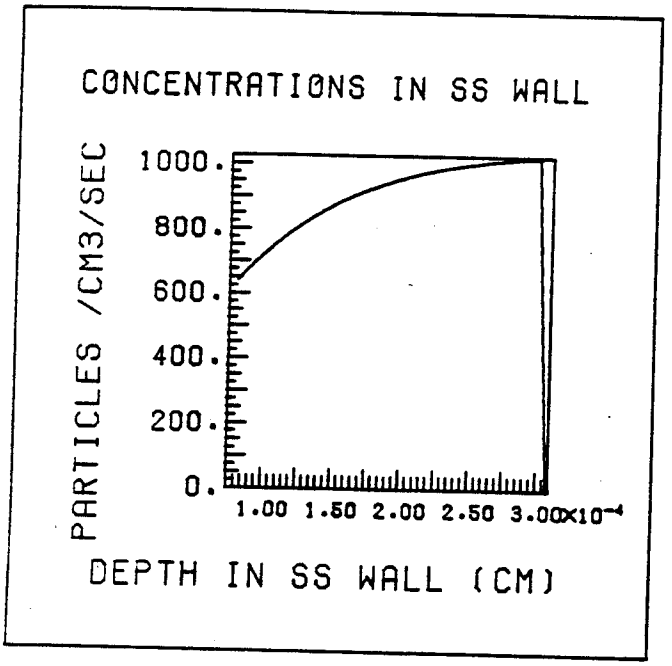

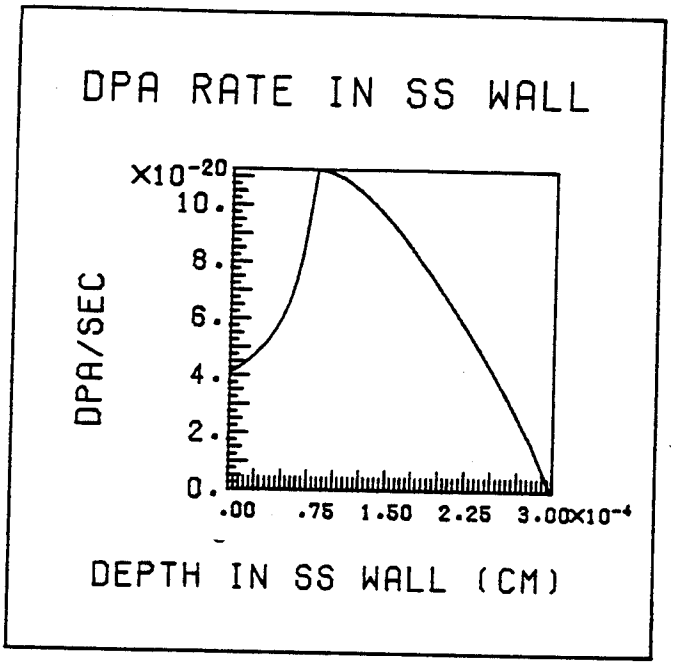

PROTONS

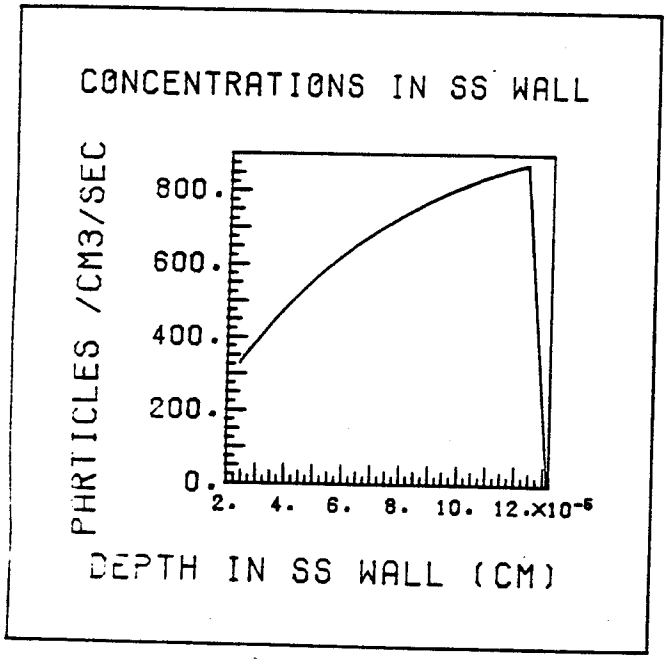

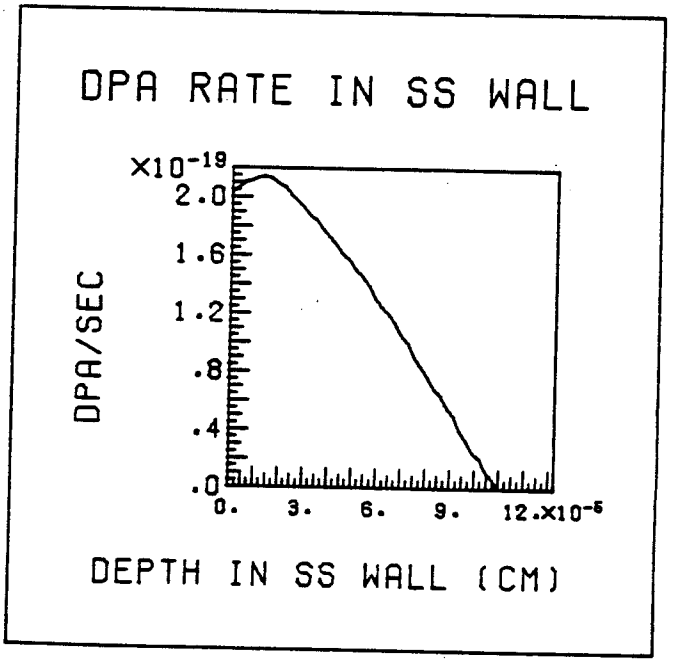

TRITIUM

Figure 10.

OUTER WALL (3.0 ATM)

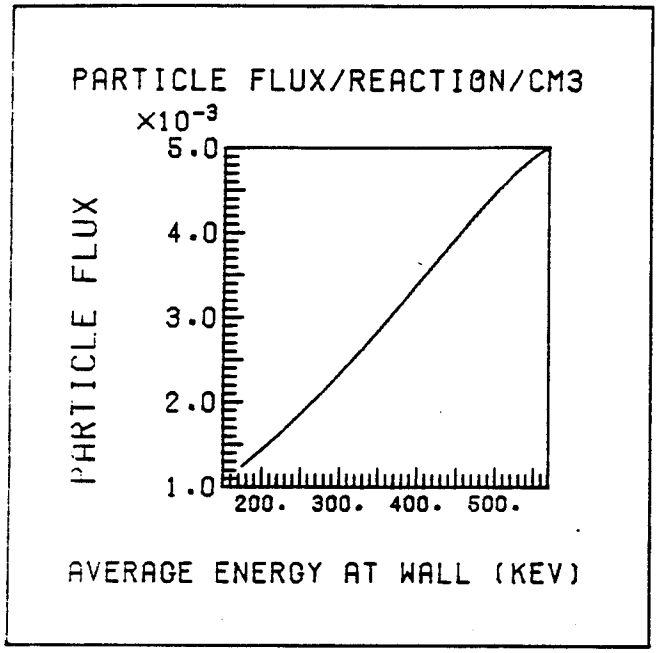

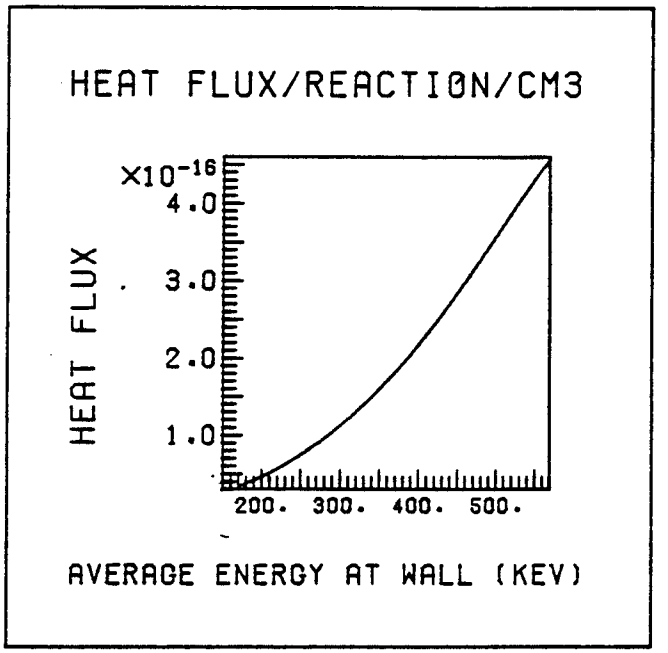

PROTONS

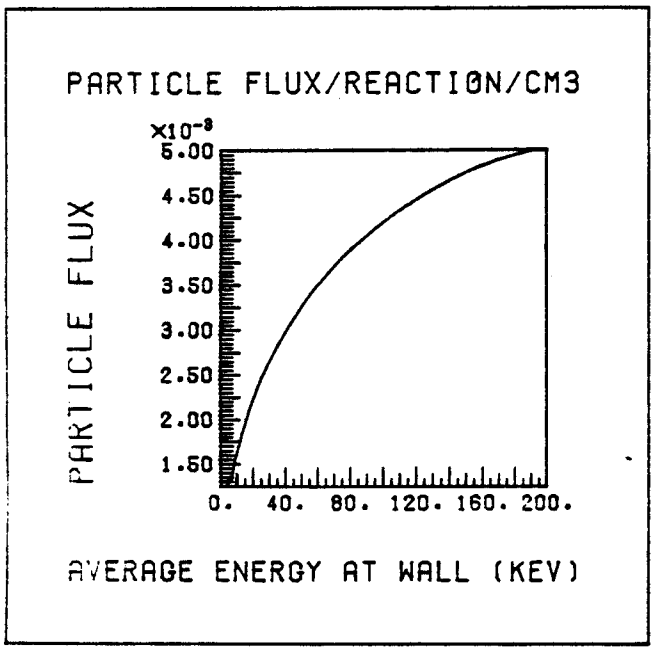

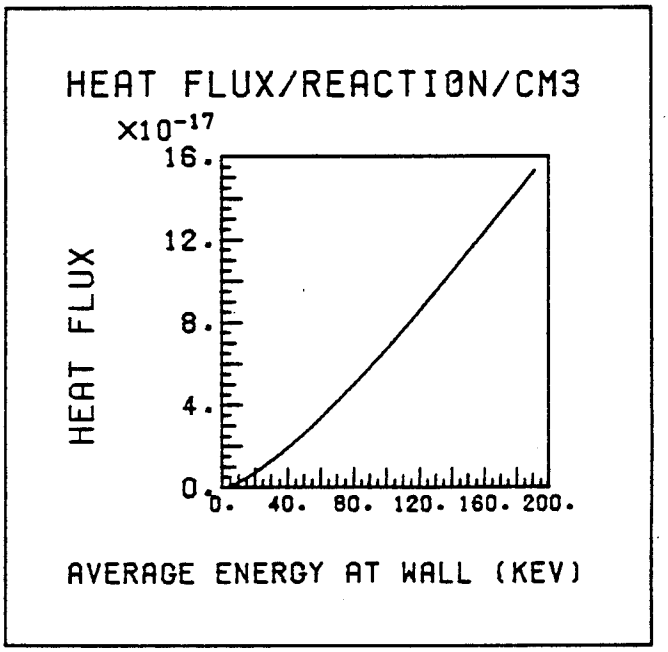

TRITIUM

Figure 11.

OUTER WALL (3.0 ATM)

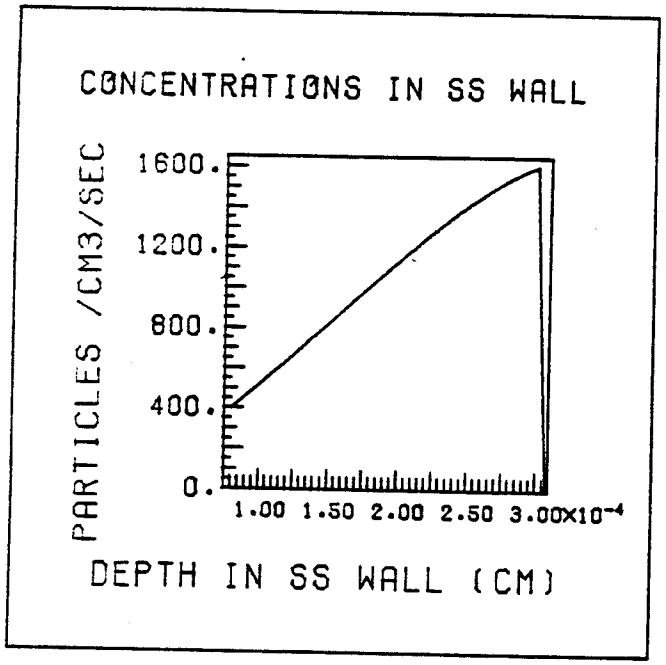

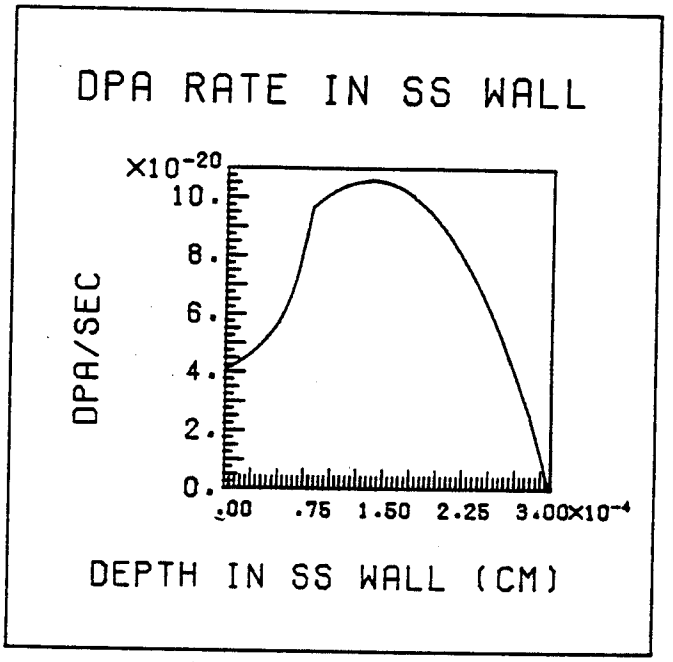

PROTONS

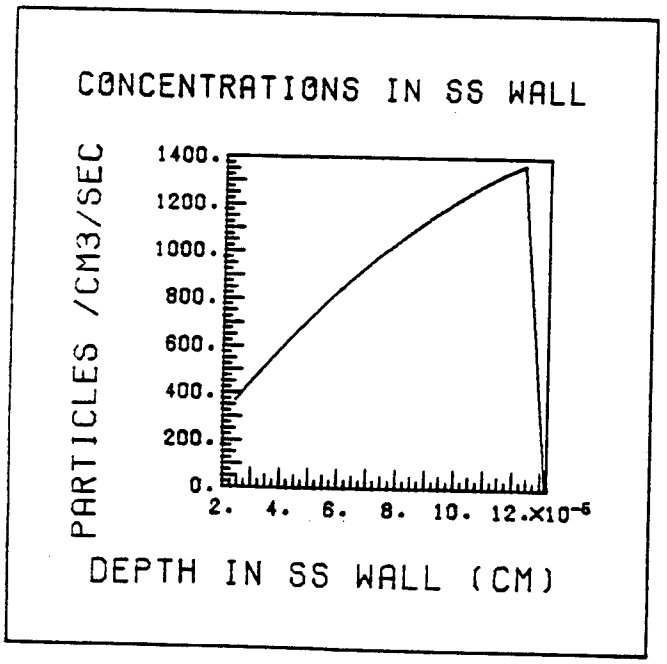

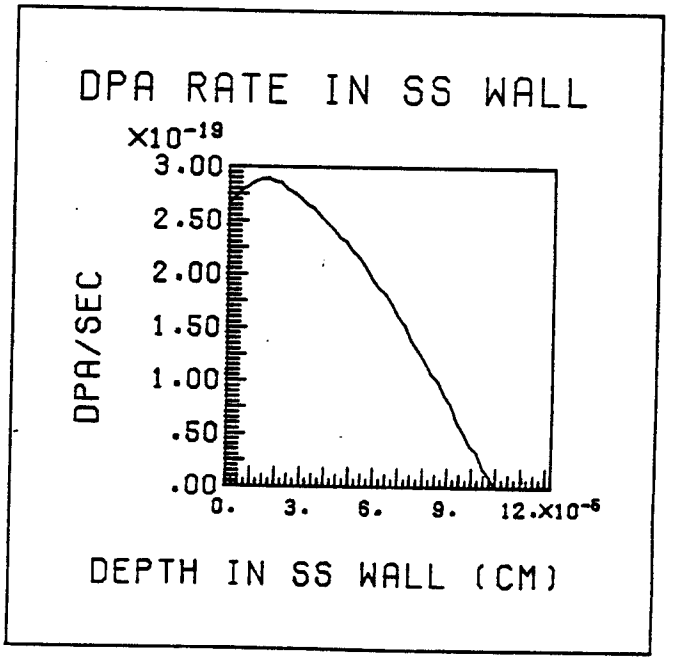

TRITIUM

Figure 12.

INNER WALL (5.0 ATM)

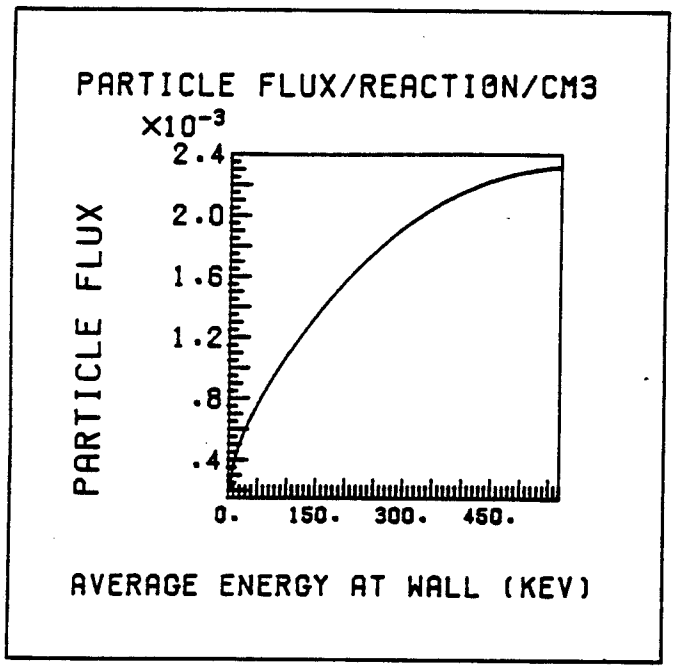

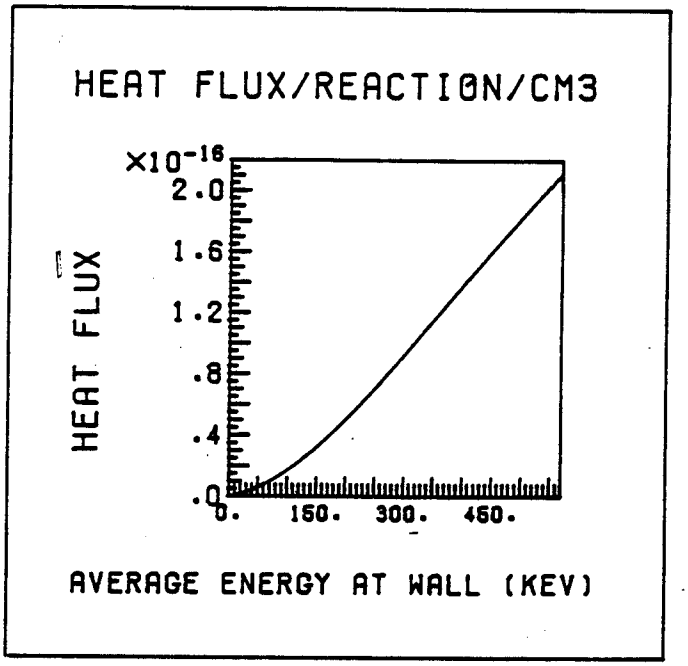

PROTONS

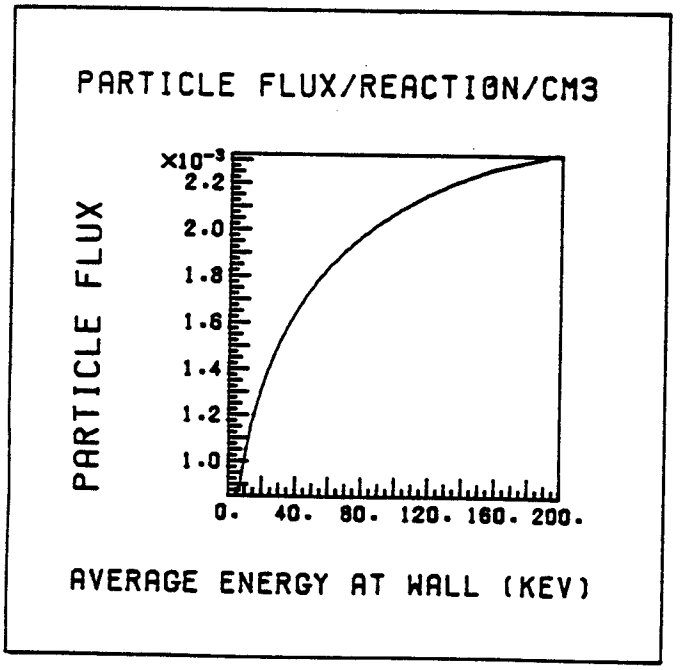

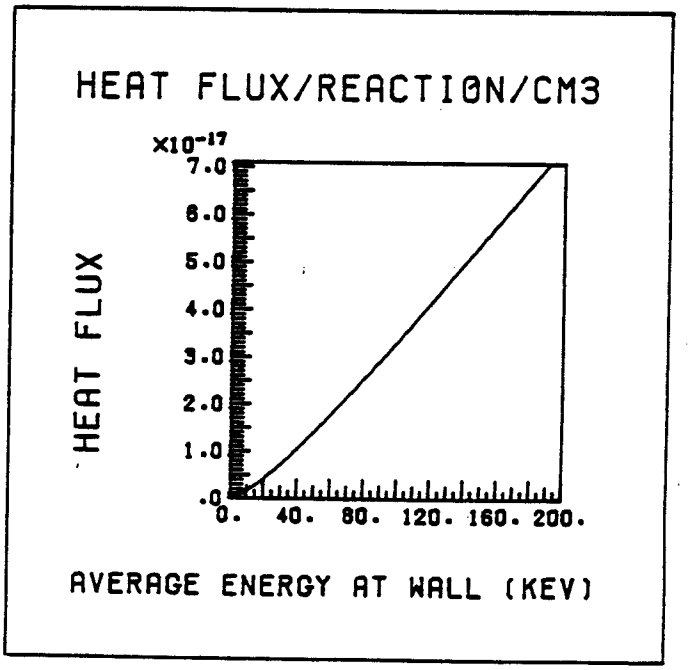

TRITIUM

Figure 13.

INNER WALL (5.0 ATM)

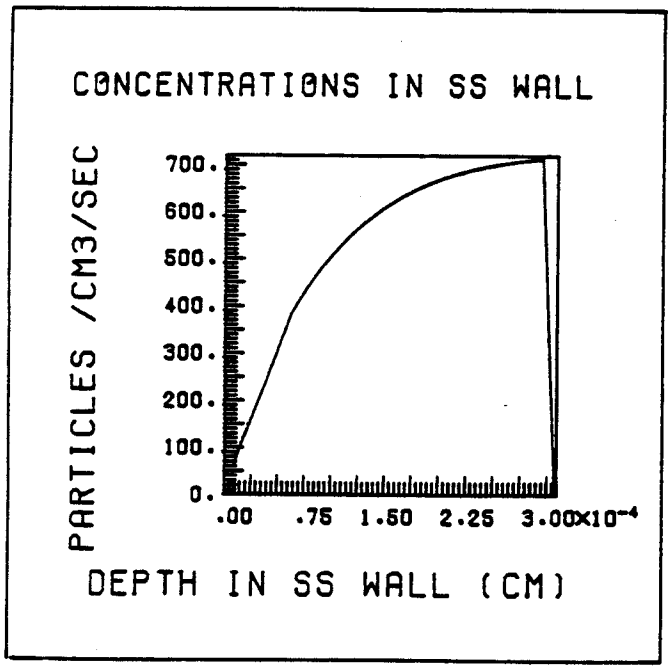

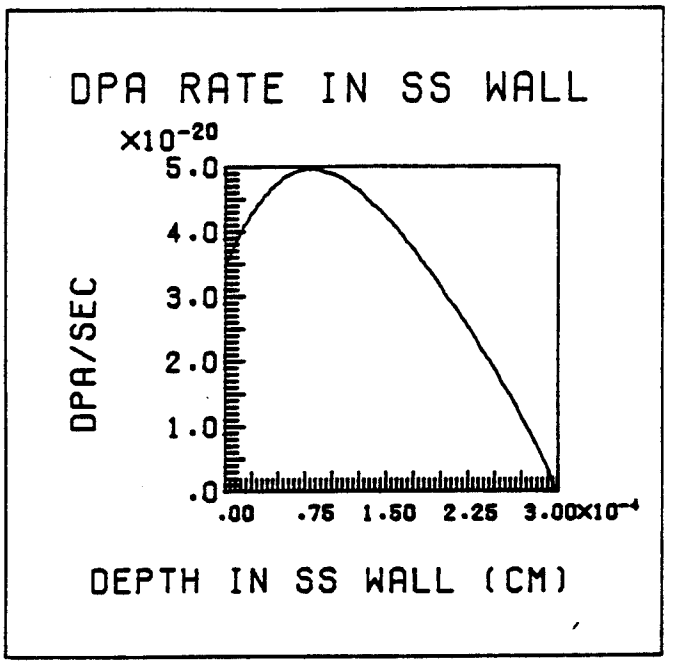

PROTONS

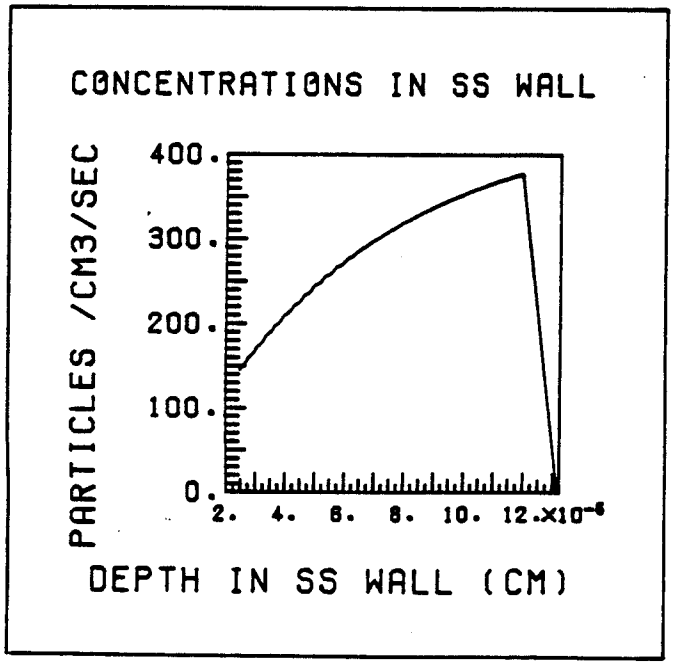

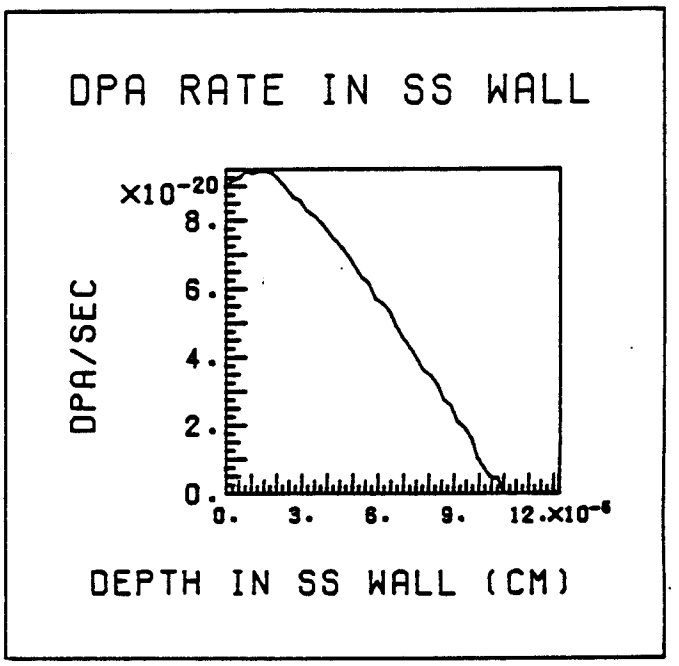

TRITIUM

Figure 14.

OUTER WALL (5.0 ATM)

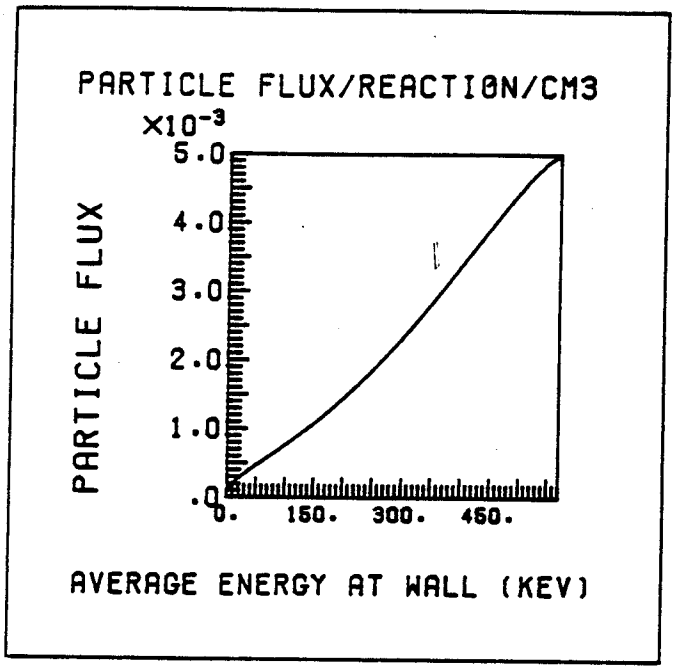

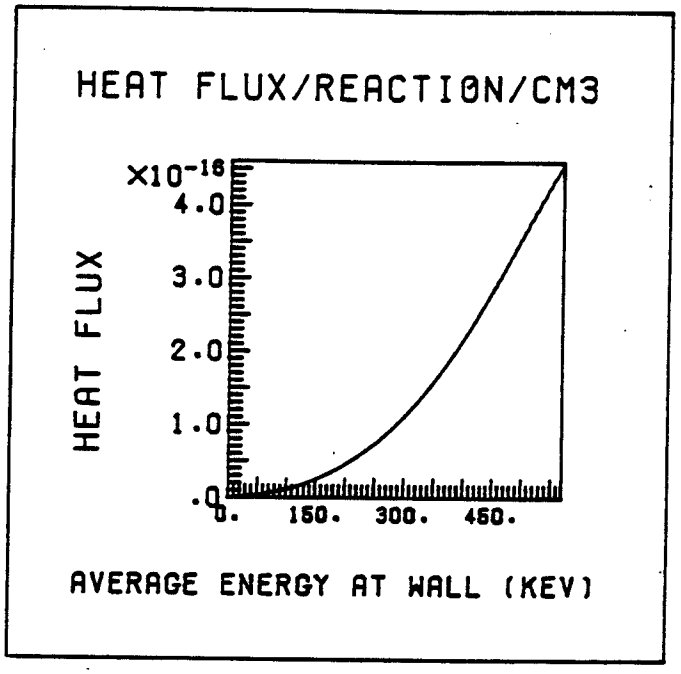

PROTONS

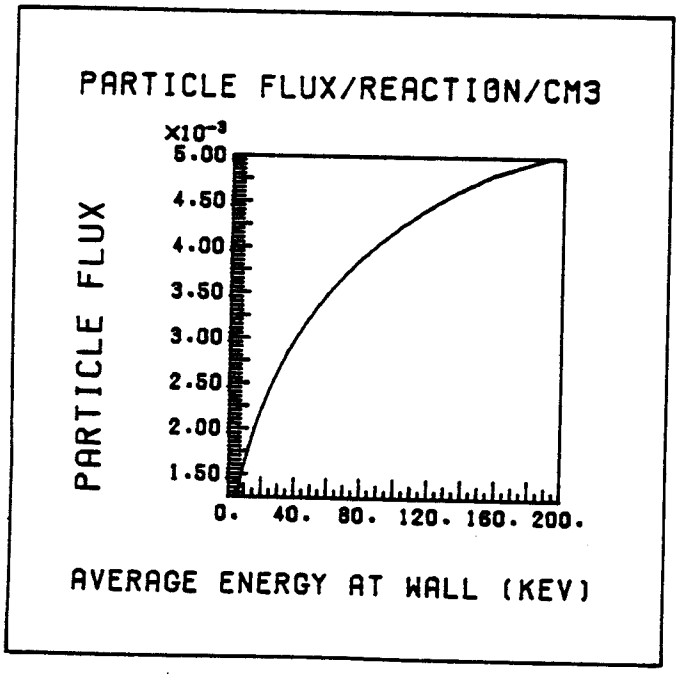

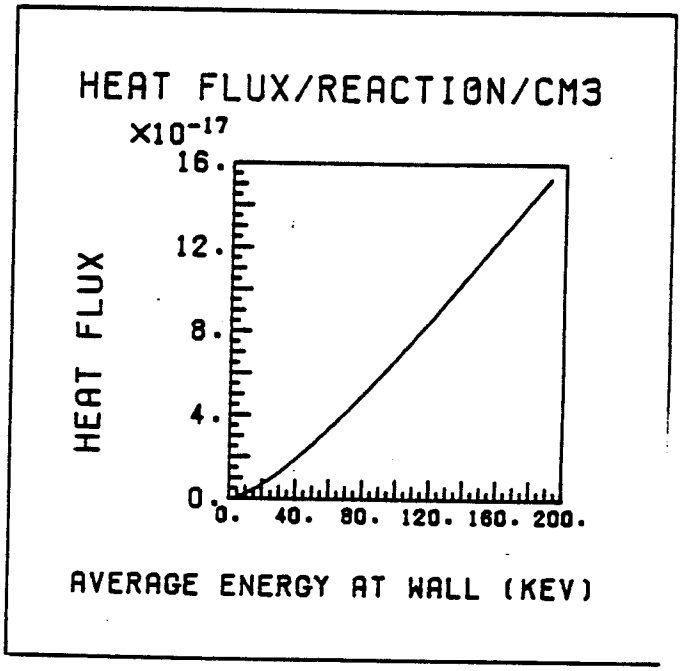

TRITIUM

Figure 15.

OUTER WALL (5.0 ATM)

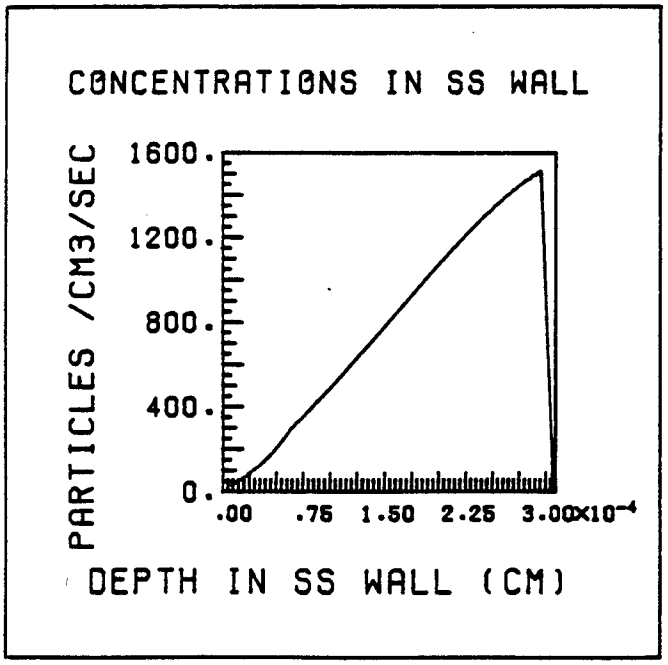

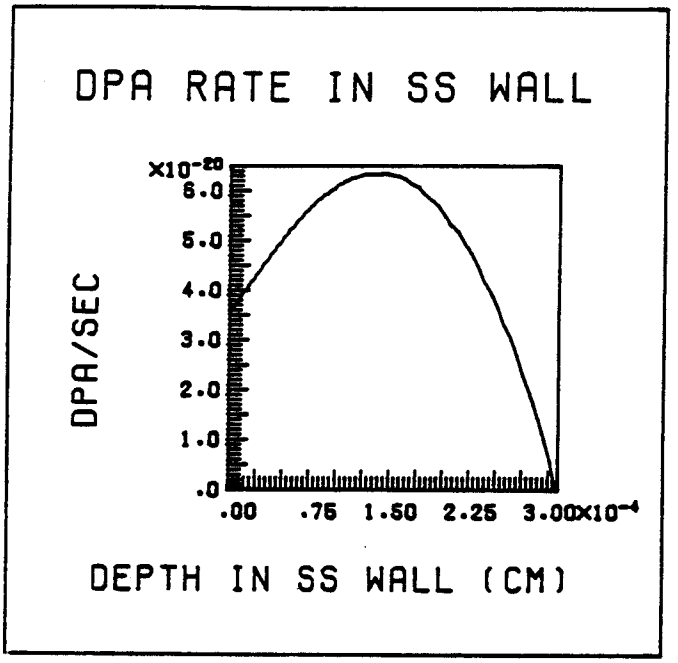

PROTONS

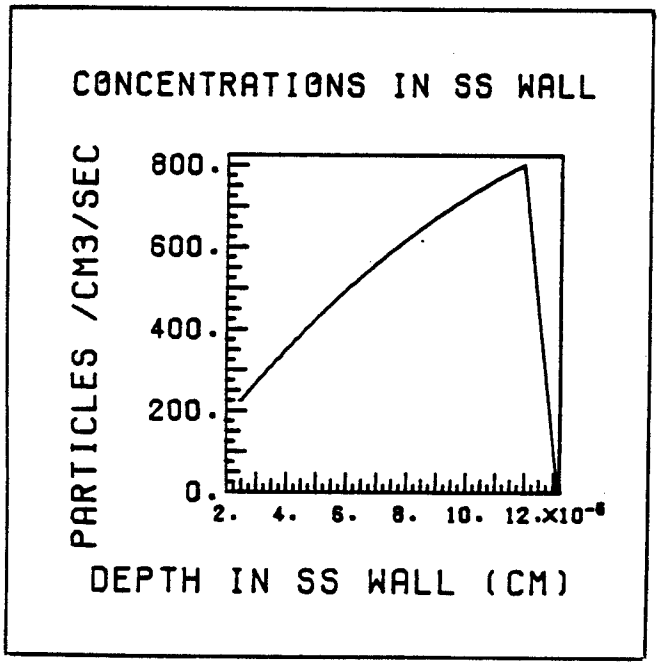

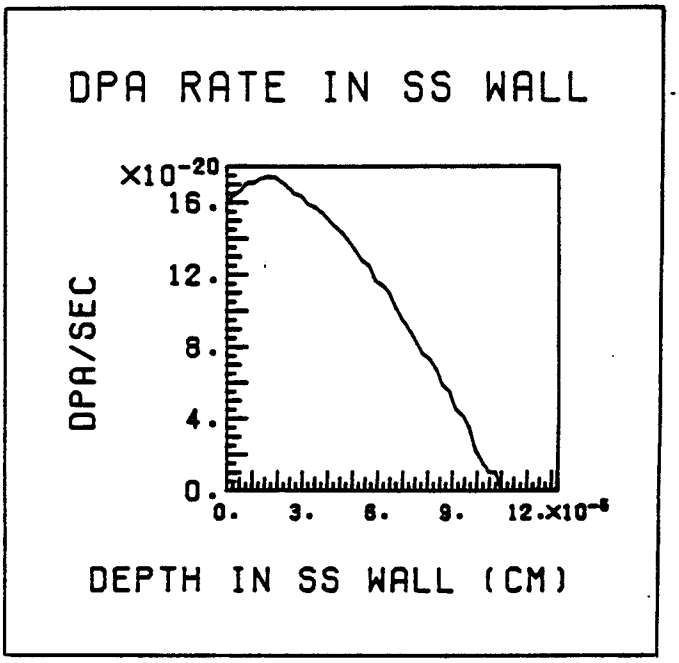

TRITIUM

Figure 16.

INNER WALL (32.7 ATM)

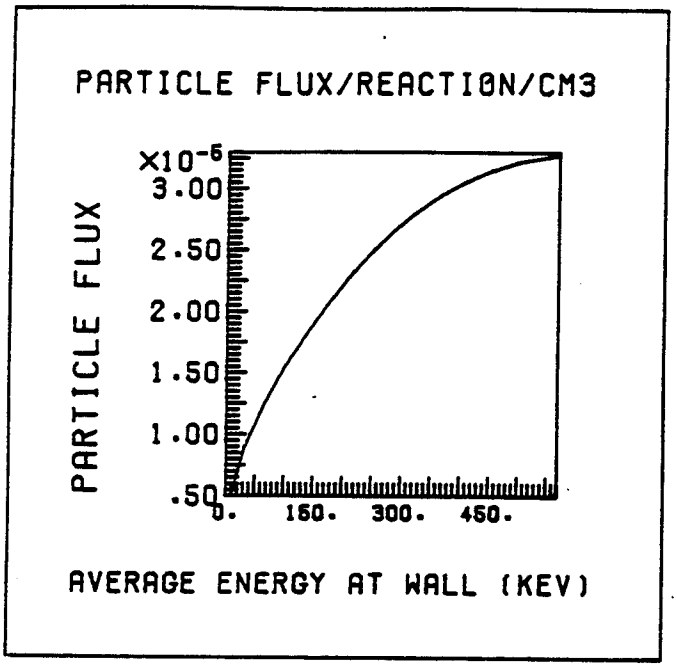

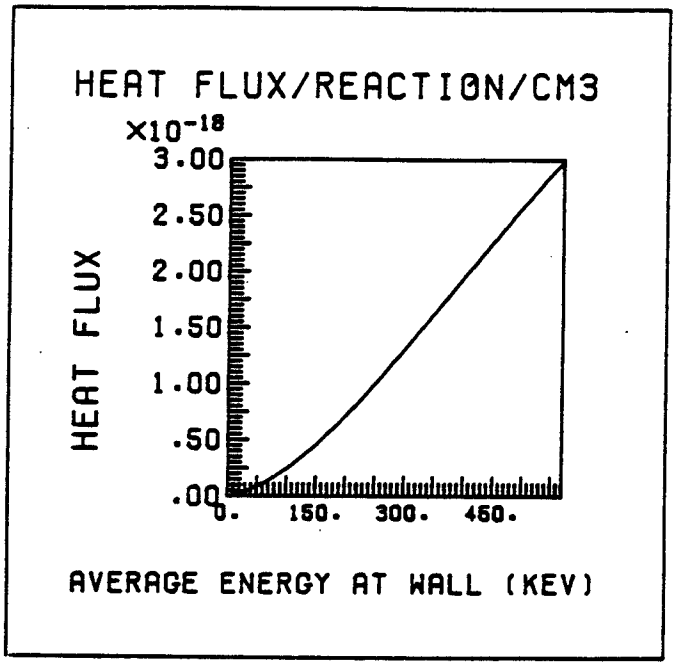

PROTONS

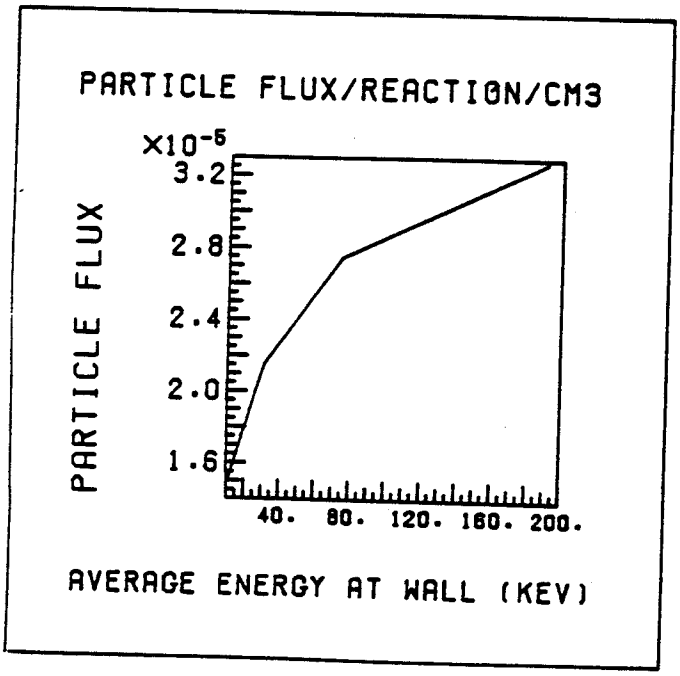

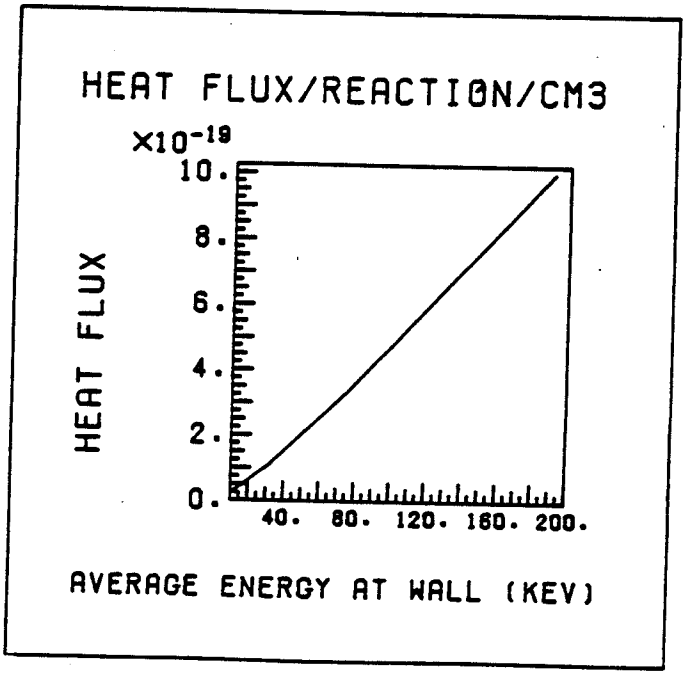

TRITIUM

Figure 17.

INNER WALL (32.7 ATM)

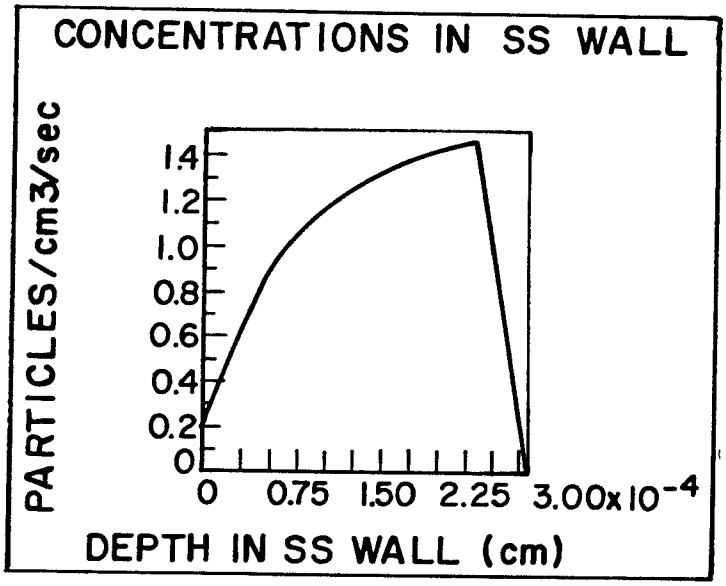

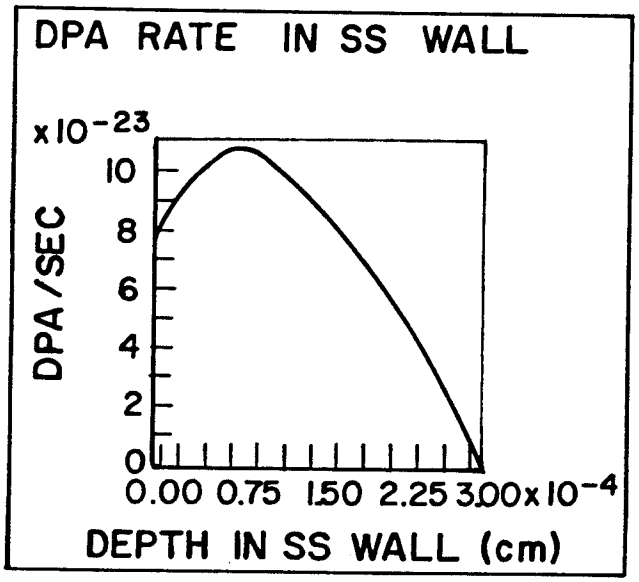

PROTONS

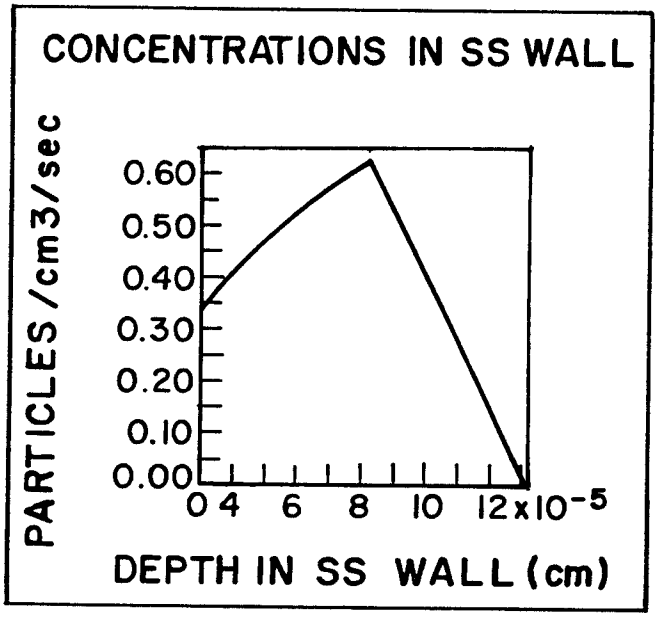

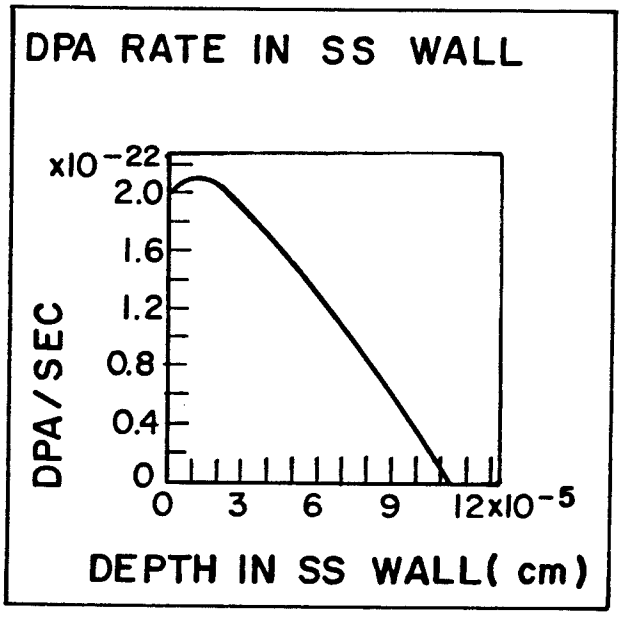

TRITIUM

Figure 18.

OUTER WALL (32.7 ATM)

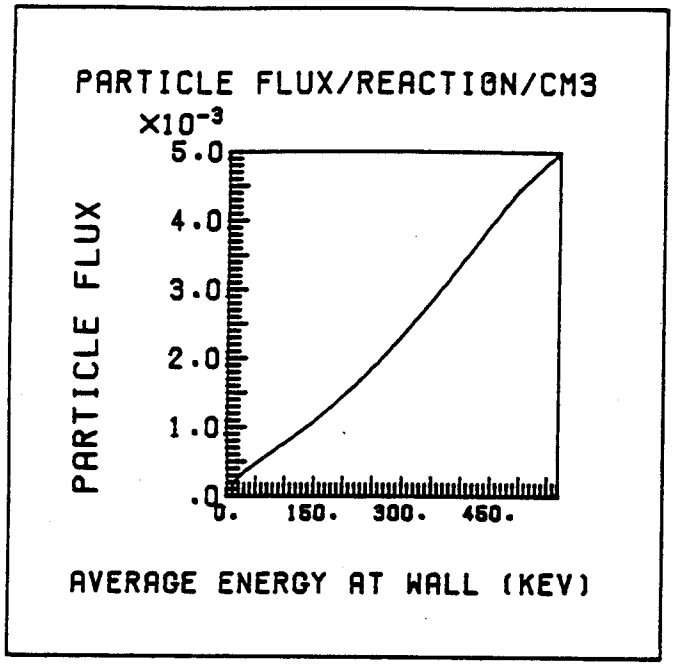

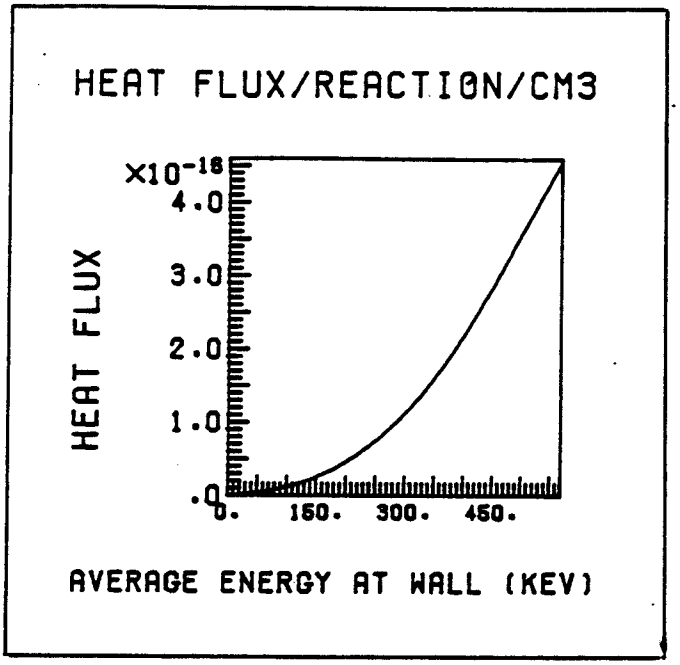

PROTONS

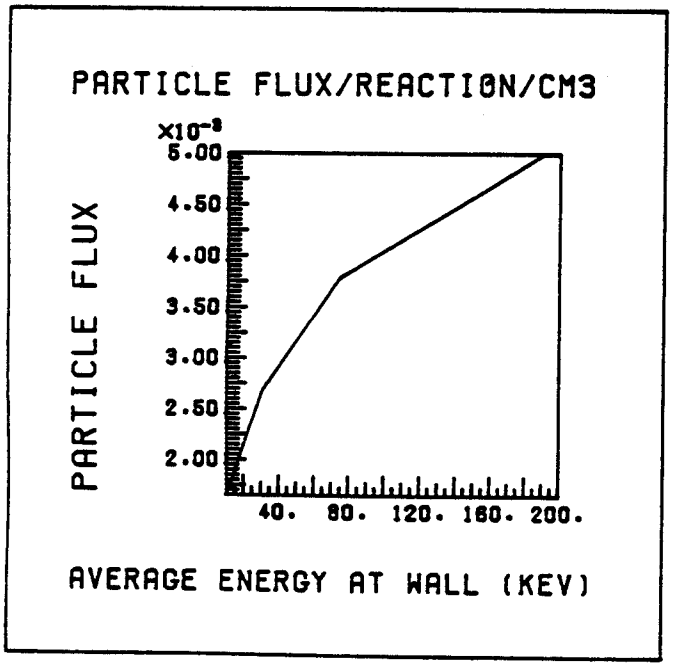

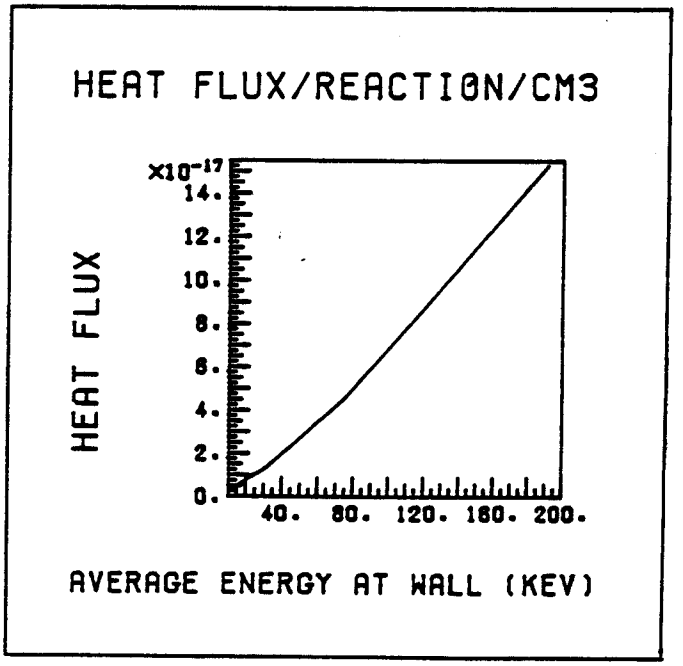

TRITIUM

Figure 19.

OUTER WALL (32.7 ATM)

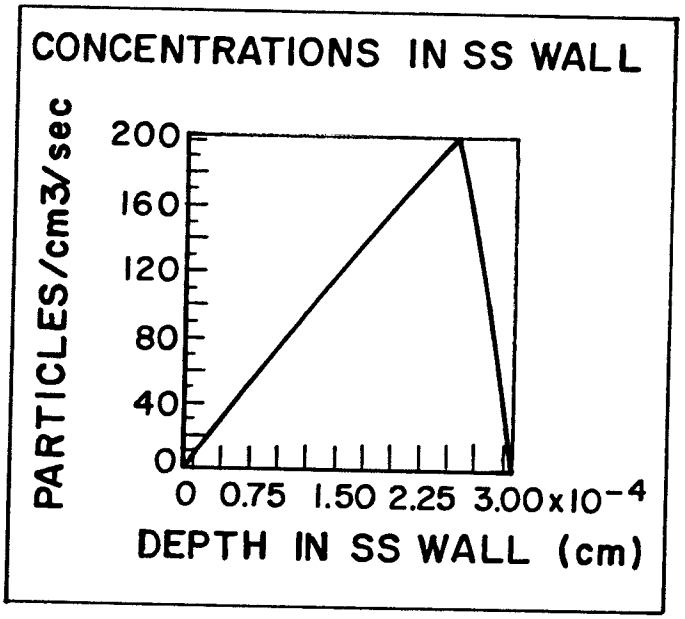

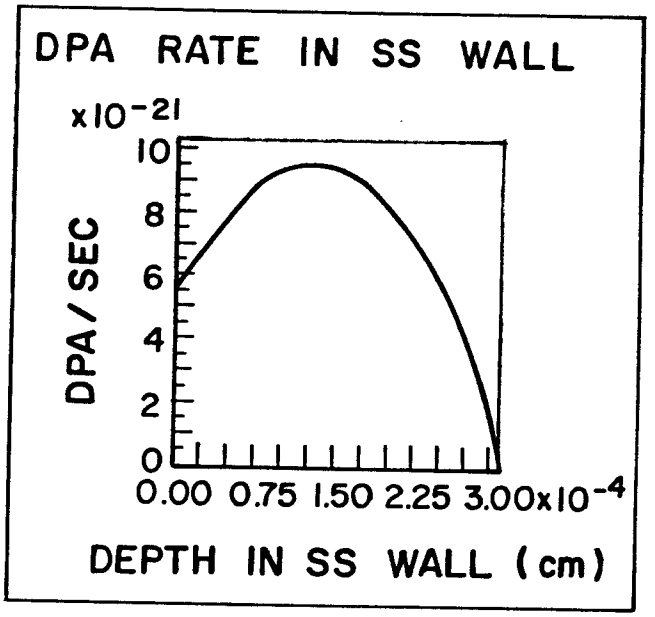

PROTONS

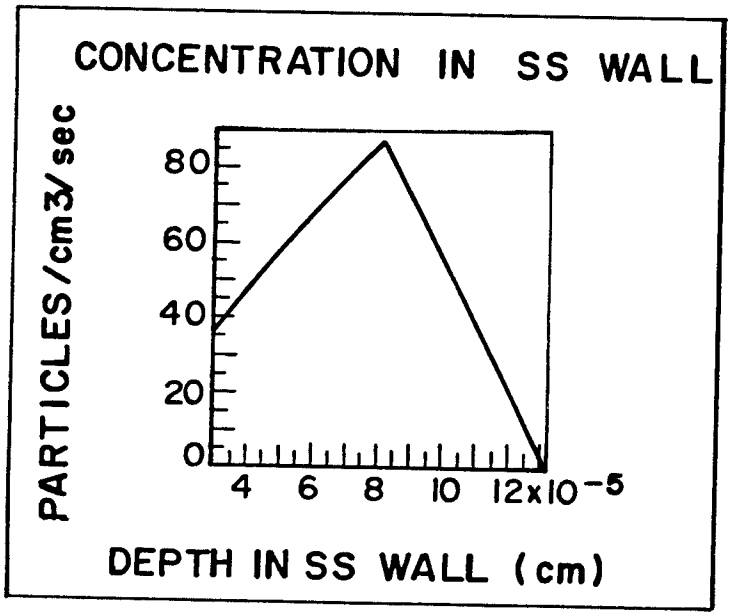

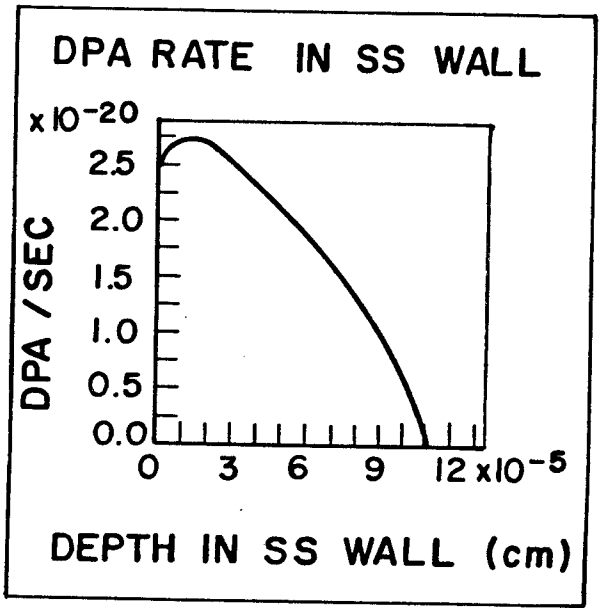

TRITIUM

Figure 20.

PROTONS

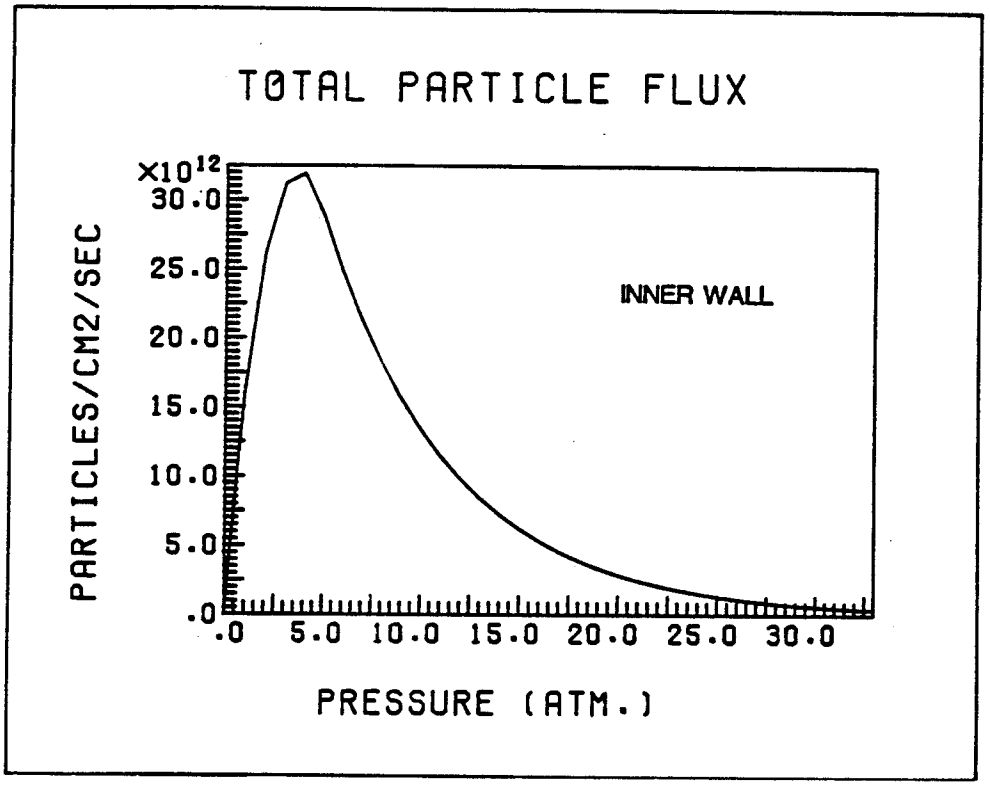

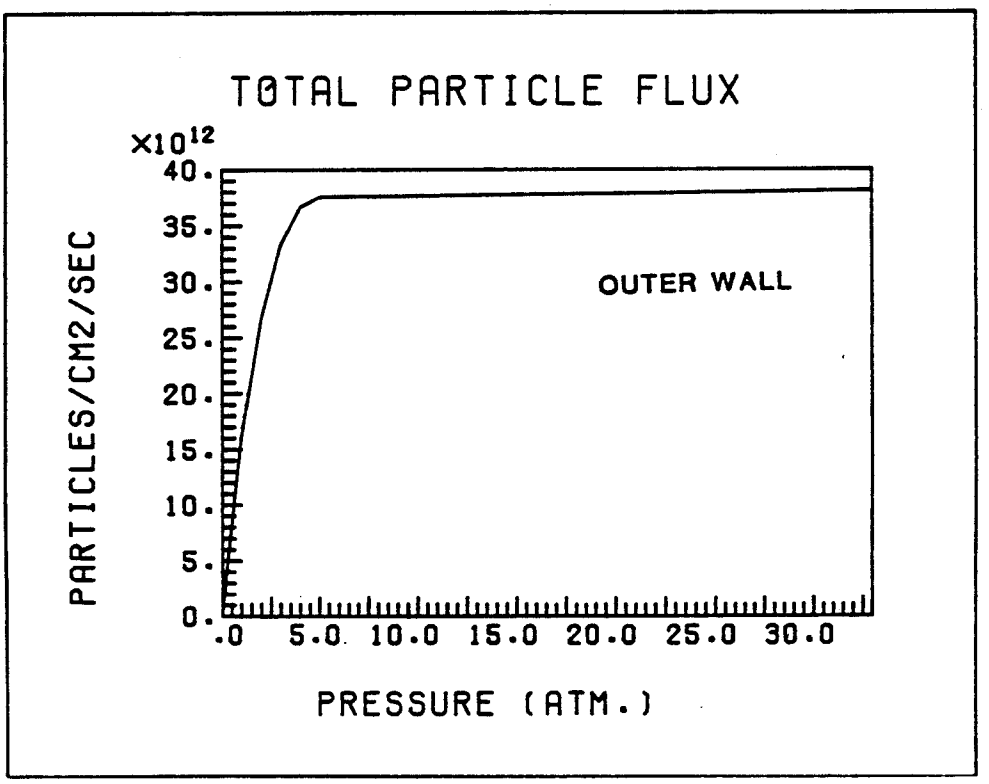

Figure 21.

PROTONS

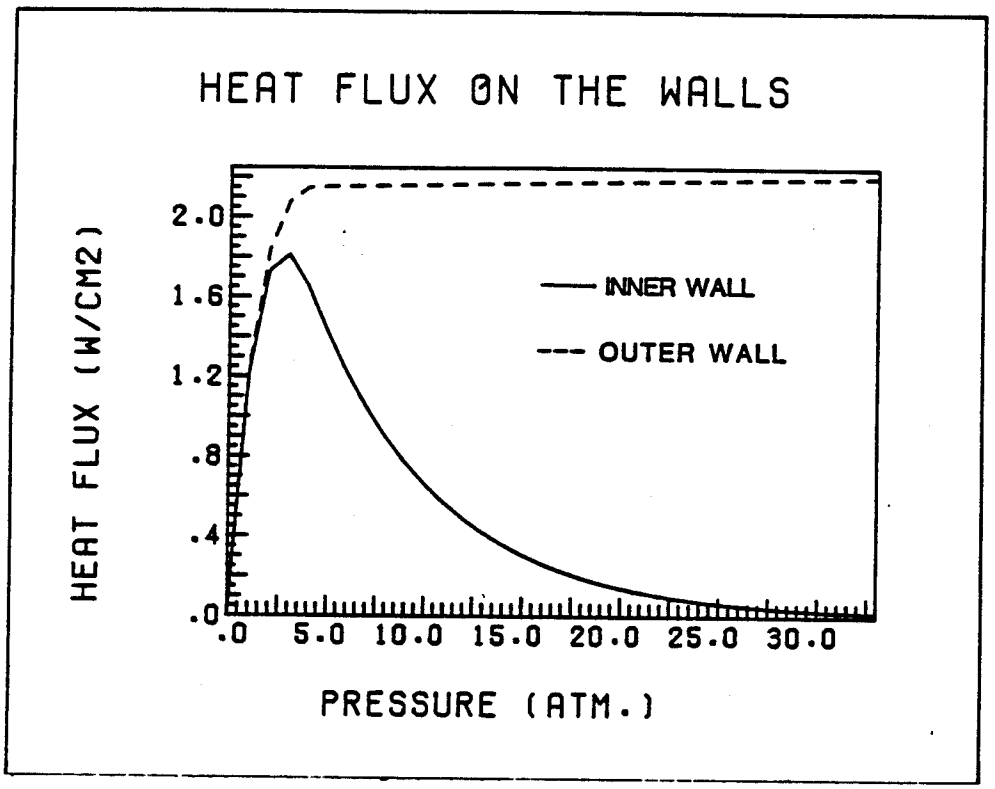

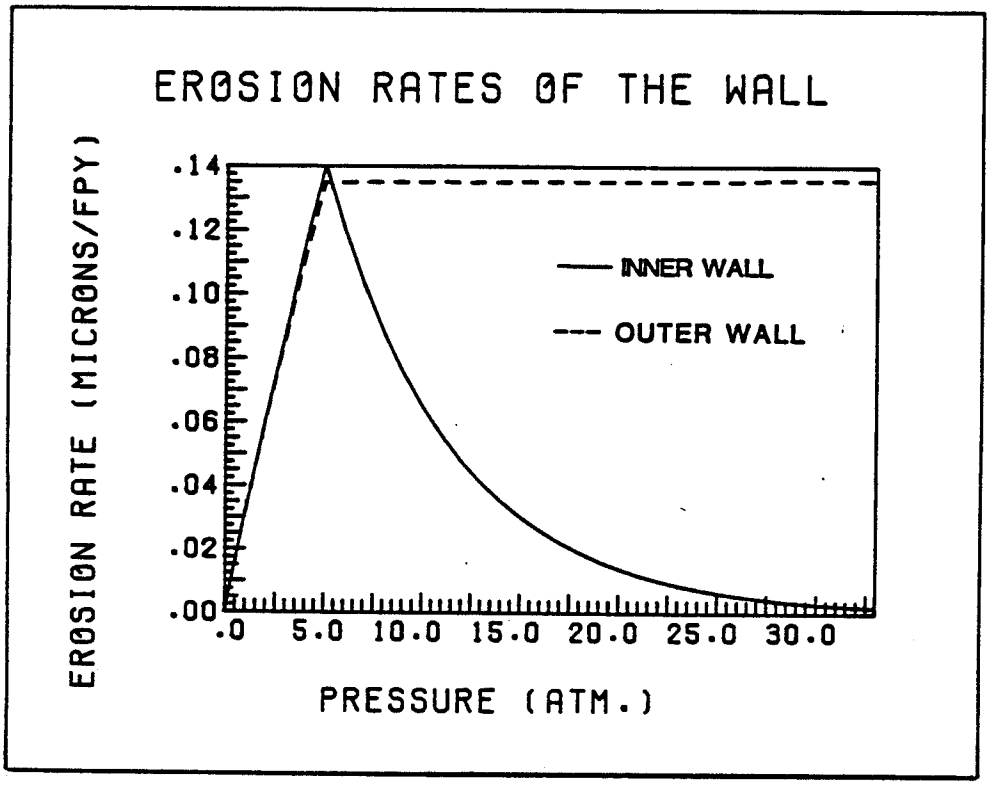

Figure 22.

TRITIUM

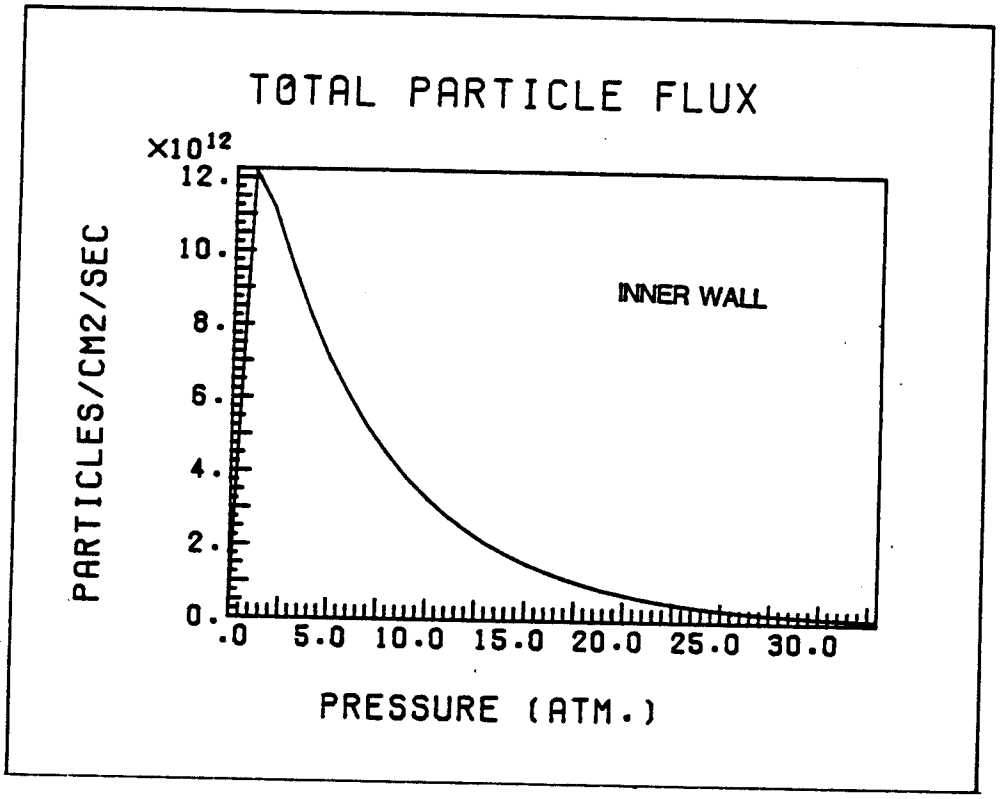

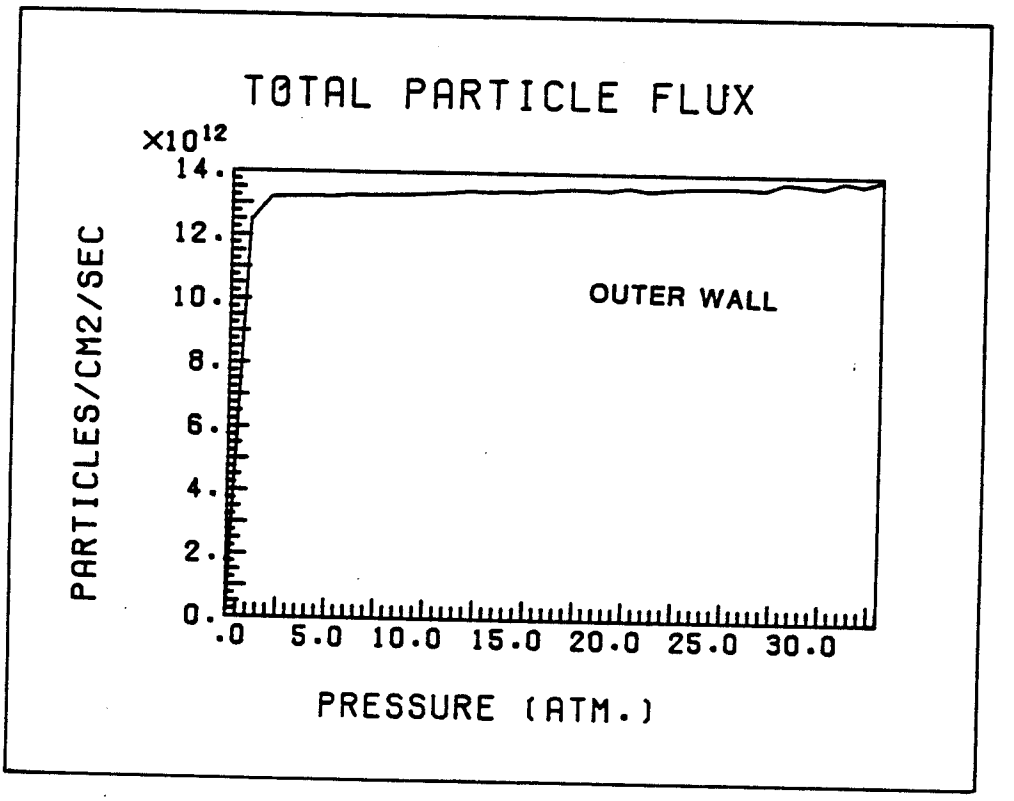

Figure 23.

TRITIUM

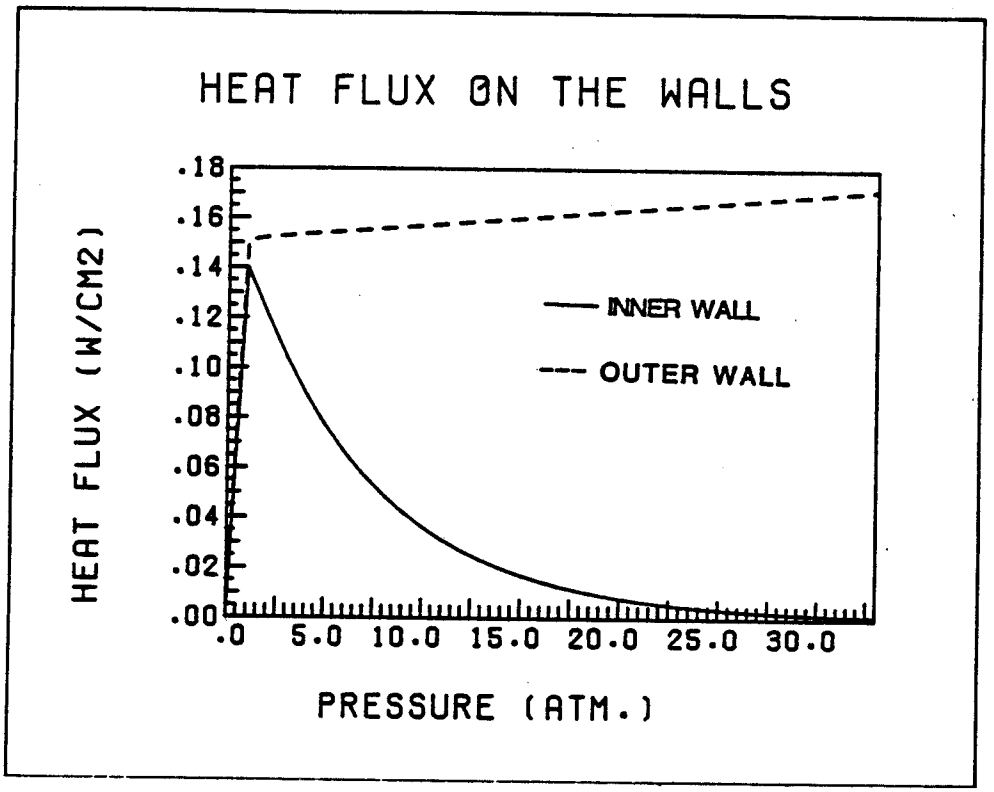

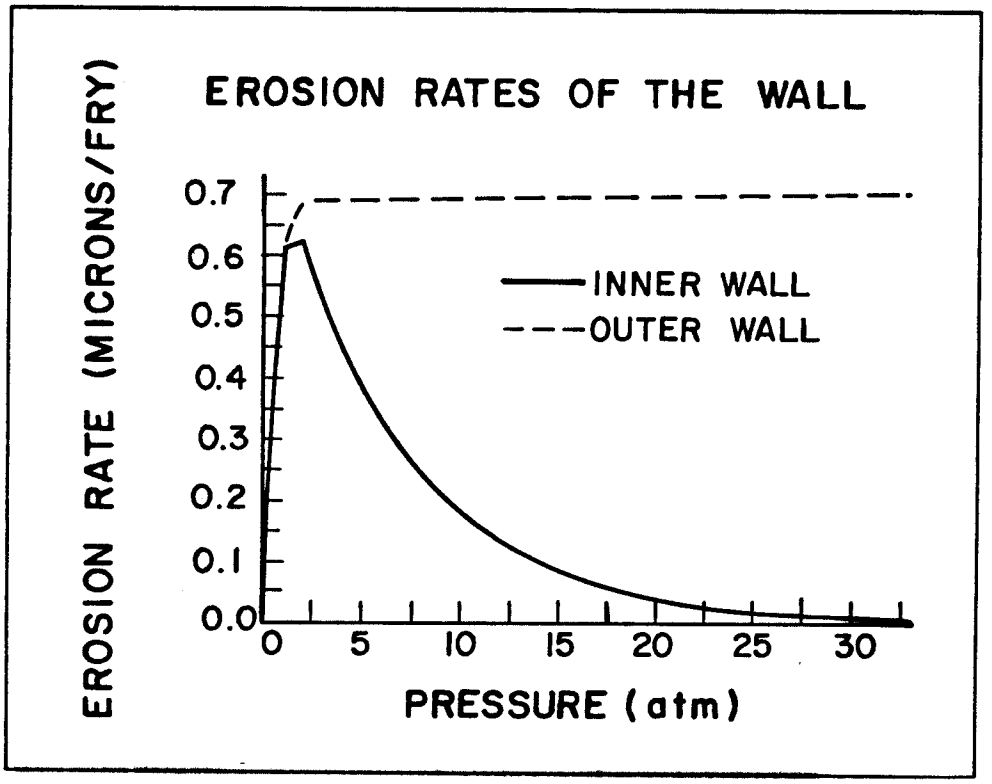

5. The particle and heat flux to the outer wall are rather insensitive to the He^3 gas pressure above 3 atm.
6. The particle and heat flux to the outer wall are higher than those to the inner wall for both protons and tritium. This is because the particle production rate due to the neutronic reaction $He^3(n,P)T$ is higher near the outer wall.

B. Erosion Rate

1. Unlike the particle and heat flux which are dominated by the protons, the erosion rate is dominated by the tritium ions. This is because of the lower energy spectrum of tritium as well as the higher sputtering coefficient which both tend to enhance the erosion rate.
2. The erosion rate for the outer wall is relatively insensitive to the gas pressure above 3 atm. In fact it increases slightly with pressure in contrast to the case for the inner wall. This is because the reaction rate is increased slightly faster than the stopping of the particles in the gas at higher pressures.
3. For protons on the inside wall (which can be seen better from tabulated data), the particle flux is maximum around 4 atm and the heat flux is maximum around 3 atm, while the erosion rate is maximum around 5 atm. This can be explained as follows. The maximum value of the heat flux depends on the product of both the particle flux and the energy spectrum of the particles at the inner wall. The energy of the particles at the inner wall is higher at lower pressures because of reduced energy loss in the gas and the particle flux is peaked around 4 atm (it is sharply decreased at lower and higher pressures). The combination of these two effects explains why the heat flux peaked around 3 atm, a value slightly

lower than the corresponding value for the peak particle flux (i.e. 4 atm). In case of the erosion rate, the maximum value is increased towards higher pressures so that the energy at the inner wall is lower and consequently the erosion rate is higher. And, again, because the particle flux decreases sharply at higher pressures, i.e., the maximum of the erosion rate is increased slightly towards higher pressures, i.e., around 5 atm.

4. In any case, for a typical ETR flux (ϕ_0 = 2.5 x 10^{14} neutrons/cm^2·sec) the total erosion rate is about 1 micron per FPY (Full Power Year) which is still very small compared to values expected in fusion reactor first walls, namely about 100 to 1000 microns/FPY.

C. Implantation

1. The maximum concentration in the inner and outer wall is near the end of the range of the protons and tritium atoms.
2. The concentration in the outside wall is about twice that of the inner wall at low pressure (5 atm) and is much higher at higher pressures (32.7 atm).
3. The maximum concentration of protons in the walls is greater than the concentration of the tritium even though the tritium range is about 3 times lower than that for protons.
4. The high concentration of protons and tritium inside both the inner and outer walls might cause blistering.

D. Damage Rate

1. Tritium dominates the highest displacement rates for both inner and outer walls.

2. The maximum dpa rate for tritium occurs almost at the surface for both walls.
3. For protons, the highest dpa rate occurs at about 0.7 micron from the surface up to 2.0 micron from the surface depending on the energy flux corresponding to a particular He^3 gas pressure.
4. A typical value for dpa rate ($\phi_o \simeq 2.5 \times 10^{14}$ neutrons/cm^2•sec) is about 4×10^{-5} dpa/sec which is about 400 times higher than that due to neutron irradiation.

VI. Conclusions

We have examined the potential for performing fusion first wall testing in a fusion reactor as proposed by Hsu et al. Preliminary results from the test case show that a number of important fusion technology issues could be tested experimentally in a fusion reactor such as ETR. In terms of particle and heat flux, we found that a layer of He^3 gas can provide a considerable amount of surface heating. The surface and bulk heating in the first wall can be correlated with He^3 pressure and reactor power to give temperature profiles similar to those expected in fusion reactors. The total erosion rate, of about 1 micron/FPY for a typical ETR flux, is still very small compared to values expected in fusion first walls. On the other hand, critical issues of high hydrogen implantation and possible causes of blistering can be examined easily with such a facility because of the high particle flux. The concept clearly warrants further study.

Acknowledgment

The authors would like to thank Dr. P. Hsu and Mr. L. G. Miller for their help and support in examining this new testing concept.

References

1. P. Y. S. Hsu, et al., Fusion Technology Development - First Wall/Blanket Systems and Component Testing in Existing Nuclear Facilities, EGG-FT-5281, December 1980, Idaho National Engineering Laboratory.

2. D. K. Brice, Physical Review A, Vol. 6. No. 5, 1791, (Nov. 1972).

3. T. O. Hunter and G. L. Kulcinski, UWFDM-217, University of Wisconsin, Madison, (Oct. 1977).

4. D. L. Smith, Trans. Am. Nucl. Soc., 27, 265, (1977).

5. P. Sigmund, Physical Review, Vol. 184, No. 2, (August 1969).

6. O. R. Olander, Fundamental Aspects of Nuclear Reactor Fuel Elements, TID-26711-P1, USERDA, 1976.

7. A. M. Hassanein and G. L. Kulcinski, to be published.